Coupled ocean-atmosphere nested modeling of the Adriatic Sea during winter and spring 2001

Julie Pullen,[1] James D. Doyle,[1] Richard Hodur,[1] Andrea Ogston,[2] Jeffrey W. Book,[3] Henry Perkins,[3] and Richard Signell[4]

[1] Realistic simulations of the Adriatic Sea for over 125 days are conducted using the Navy Coastal Ocean Model with atmospheric forcing provided by the Coupled Ocean/Atmosphere Mesoscale Prediction System (COAMPS is a registered trademark of the Naval Research Laboratory (COAMP™)). In two separate simulations of the Adriatic, a nested 2-km-resolution ocean model is forced by the inner (4-km) and outer (36-km) nests of the atmospheric model. Two meteorological stations and two acoustic Doppler current profiler observation sites are used to evaluate modeled atmosphere and ocean velocity fields for 28 January–4 June 2001. Modeled/observed correlations of atmospheric 10-m velocity are greater than 0.85 for both resolution models. Oceanic 5- and 25-m current fluctuations from both simulations generally match the magnitude and orientation of the observations. The 4-km-resolution atmospheric model is differentiated from the 36-km-resolution model by its ability to resolve the small-scale flow structures of the "bora" wind and by its better agreement with observed wind velocity statistics. The ocean simulation forced by the 4-km-resolution model is distinguished from the one forced by the 36-km-resolution model by its ability to reproduce the expected double-gyre circulation in the northern Adriatic and by its ability to better capture the magnitude and shape of the observed depth-dependent velocity correlation with wind at the deeper site. Though the 36-km forced ocean model agrees better with many observed velocity statistics, the 4-km forced ocean model produces the highest correlations with observations (exceeding 0.78) at subsurface depths that are most strongly correlated with winds. *INDEX TERMS:* 3339 Meteorology and Atmospheric Dynamics: Ocean/atmosphere interactions (0312, 4504); 4263 Oceanography: General: Ocean prediction; 4247 Oceanography: General: Marine meteorology; 4243 Oceanography: General: Marginal and semienclosed seas; *KEYWORDS:* Adriatic Sea, ocean-atmosphere interaction, high-resolution modeling, nested modeling, model validation

Citation: Pullen, J., J. D. Doyle, R. Hodur, A. Ogston, J. W. Book, H. Perkins, and R. Signell, Coupled ocean-atmosphere nested modeling of the Adriatic Sea during winter and spring 2001, *J. Geophys. Res.*, *108*(C10), 3320, doi:10.1029/2003JC001780, 2003.

1. Introduction

[2] The shallow waters of the northern Adriatic Sea are subjected to rapidly varying hydrological and meteorological forcing. The Po River is the major contributor of freshwater runoff and is given to intense flooding [*Raicich*, 1994]. The buoyant river water and extreme episodic gusts of the bora (northeasterly) and scirocco (southeasterly) winds frequently induce complex circulation in the Adriatic.

[3] Recent modeling work in the Adriatic Sea has centered on realistically configured ocean models driven by climatological coarse-resolution forcing to elucidate seasonal circulation [*Zavatarelli et al.*, 2002; *Zavatarelli and Pinardi*, 2003] or driven by short idealized forcing to illuminate process-oriented dynamics [*Bergamasco et al.*, 1999; *Kourafalou*, 2001]. They have detailed major seasonal variations like the enhanced barotropic nature of the West Adriatic Current (WAC) in winter [*Zavatarelli et al.*, 2002], and local processes like the formation of northern Adriatic deep water in winter and its transport along the west coast of the Adriatic [*Bergamasco et al.*, 1999; *Zavatarelli and Pinardi*, 2003]. However, these studies were not designed to create verifiable predictions concerning the state of the sea at a given time.

[4] In an exception to this trend, *Paklar et al.* [2001] employed a 9-km-resolution mesoscale atmospheric model to force an Adriatic Sea simulation of 5-day duration. The goal of their work was to reproduce a satellite Sea Surface Temperature (SST) image of Po River water wrapping into a cyclonic gyre in the far northern Adriatic. The offshore excursion of the Po plume in the satellite image stands in contrast to typical winter conditions where the Po plume is confined to the western Adriatic shelf region [*Sturm et al.*,

[1]Marine Meteorology Division, Naval Research Laboratory, Monterey, California, USA.
[2]School of Oceanography, University of Washington, Seattle, Washington, USA.
[3]Naval Research Laboratory, Stennis Space Center, Mississippi, USA.
[4]SACLANT Undersea Research Centre, La Spezia, Italy.

Report Documentation Page

Public reporting burden for the collection of information is estimated to average 1 hour per response, including the time for reviewing instructions, searching existing data sources, gathering and maintaining the data needed, and completing and reviewing the collection of information. Send comments regarding this burden estimate or any other aspect of this collection of information, including suggestions for reducing this burden, to Washington Headquarters Services, Directorate for Information Operations and Reports, 1215 Jefferson Davis Highway, Suite 1204, Arlington VA 22202-4302. Respondents should be aware that notwithstanding any other provision of law, no person shall be subject to a penalty for failing to comply with a collection of information if it does not display a currently valid OMB control number.

1. REPORT DATE **19 MAY 2003**	2. REPORT TYPE	3. DATES COVERED **00-00-2003 to 00-00-2003**

4. TITLE AND SUBTITLE **Coupled ocean-atmosphere nested modeling of the Adriatic Sea during winter and spring 2001**	5a. CONTRACT NUMBER
	5b. GRANT NUMBER
	5c. PROGRAM ELEMENT NUMBER
6. AUTHOR(S)	5d. PROJECT NUMBER
	5e. TASK NUMBER
	5f. WORK UNIT NUMBER
7. PERFORMING ORGANIZATION NAME(S) AND ADDRESS(ES) **Naval Research Laboratory,7 Grace Hopper Ave., Stop 2 ,Monterey,CA,93943-5502**	8. PERFORMING ORGANIZATION REPORT NUMBER
9. SPONSORING/MONITORING AGENCY NAME(S) AND ADDRESS(ES)	10. SPONSOR/MONITOR'S ACRONYM(S)
	11. SPONSOR/MONITOR'S REPORT NUMBER(S)

12. DISTRIBUTION/AVAILABILITY STATEMENT **Approved for public release; distribution unlimited**

13. SUPPLEMENTARY NOTES

14. ABSTRACT

15. SUBJECT TERMS

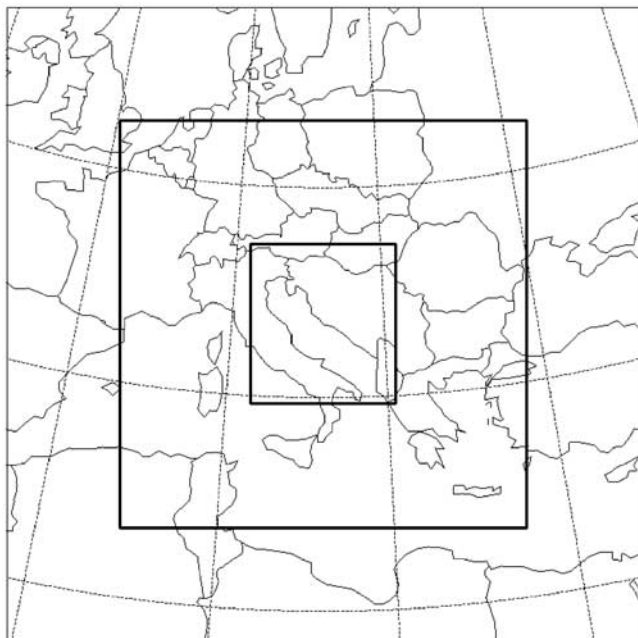| 16. SECURITY CLASSIFICATION OF:			17. LIMITATION OF ABSTRACT	18. NUMBER OF PAGES	19a. NAME OF RESPONSIBLE PERSON
a. REPORT **unclassified**	b. ABSTRACT **unclassified**	c. THIS PAGE **unclassified**	**Same as Report (SAR)**	**20**	

Figure 1. Nested grid domain for the atmospheric COAMPS model reanalysis. Nested grids of 36, 12, and 4 km (delineated with thick black lines) were configured for a simulation with 30 sigma levels. The innermost (4-km) grid has 187×205 horizontal cells.

1992]. By examining the results of the impact of combinations of wind stress, heat flux, and river runoff on a 5-km-resolution implementation of the Princeton Ocean Model with 16 sigma levels and realistic bathymetry, the authors establish that all three forcing mechanisms are important for generating the remotely sensed circulation feature.

[5] The modeling results of *Paklar et al.* [2001] along with prior highly simplified modeling studies [*Kuzmic and Orlic*, 1987; *Orlic et al.*, 1994] as well as observations [*Zore-Armanda and Gacic*, 1987; *Supic et al.*, 2000; *Mauri and Poulain*, 2001] suggest that the wind stress curl applied by the bora induces a double gyre in the northern Adriatic Sea, with a cyclonic gyre occupying the shallow northern Adriatic and an anticyclone situated immediately to the south off the Istrian peninsula. The Po River plume appears to simply be entrained into the circulation of the northern cyclonic gyre. The analysis of satellite images by *Sturm et al.* [1992] indicates that this behavior by the plume occurs following prolonged intense bora events. Though *Paklar et al.* [2001] made use of high-resolution forcing, they simulated the ocean dynamics for only 5 days. The brief model simulation was not sufficient to infer substantial information about the frequency and duration of the dominant circulation patterns.

[6] *Poulain* [2001] quantified statistically the mean and fluctuating surface circulation of the Adriatic Sea from 9 years of drifter observations. In particular, he established that the mean speed of the WAC core is 20–35 cm/s with a width of 45–60 km, depending on the season. In addition, the mean field reveals broad westward directed circulation south of the Istrian peninsula and at the steep bathymetric slope of the Jabuka Pit. In the mean there is an isolated

cyclonic gyre in the shallow waters of the northern Adriatic. The variability of the flow field is larger and more isotropic in the region where the Po River enters the sea. Variance ellipses are elongated in the coastal currents along the northern and western coasts, with standard deviations reaching the order of magnitude of the mean in these energetic regions.

[7] The overall aim of our modeling studies is to investigate in a quantitative manner the response of the northern Adriatic Sea to realistic high-resolution atmospheric forcing. We carry out the first long-term model evaluation effort for the Adriatic Sea using acoustic Doppler current profiler (ADCP) velocity observations collected during January–June 2001 by the European Strata Formation on Margins (EuroSTRATAFORM) program and by the pilot phase of the Naval Research Laboratory (NRL) Adriatic Circulation Experiment (ACE).

[8] This modeling work is designed to assist in the planning and interpretation of an ongoing suite of observations in the Adriatic Sea started in fall 2002. EuroSTRATA-FORM and ACE observations include bottom-mounted ADCPs, moored buoys, and Conductivity-Temperature-Depth (CTD) sections. Additional measurements using surface radar, airborne salinity mapping, towed undulating vehicles, and drifter releases are being conducted as well. The observational programs will generate much needed data concerning the circulation of this shallow sea subjected to river floods and strong wind events.

[9] The specific goals of the work presented here are to compare the oceanic and atmospheric modeled velocity fields with observations and to statistically document and analyze the canonical wind pattern and resultant oceanic flow. In addition, we seek to quantify the impact that the atmospheric model resolution has on the model circulation and correspondence with observations, in both the ocean and atmosphere. To achieve these goals requires attaining very high resolution in the application of the models of the atmosphere and ocean. The system we have configured is designed to resolve processes operative on small scales in both realms.

[10] This paper presents the model configuration and model forcing in sections 2 and 3. In sections 4 and 5, modeled atmospheric wind velocity and oceanic current velocities are compared to observations. In section 6 the ocean and atmosphere model results are enlisted to examine the effects of meteorological forcing on the ocean at locations removed from the measurement sites. The discussion and conclusions are presented in section 7.

2. Model Configuration

[11] We conduct simulations of the Adriatic Sea using the Navy Coastal Ocean Model (NCOM). NCOM is a hybrid sigma/z-level primitive equation, free-surface model invoking the hydrostatic, incompressible, and Boussinesq approximations [*Martin*, 2000]. The Mellor-Yamada level 2.5 turbulence scheme and Smagorinsky horizontal diffusion are utilized.

[12] Surface forcing is provided by the atmospheric component of the Coupled Ocean/Atmosphere Mesoscale Prediction System (COAMPS) [*Hodur*, 1997]. The COAMPS atmospheric model is fully compressible and
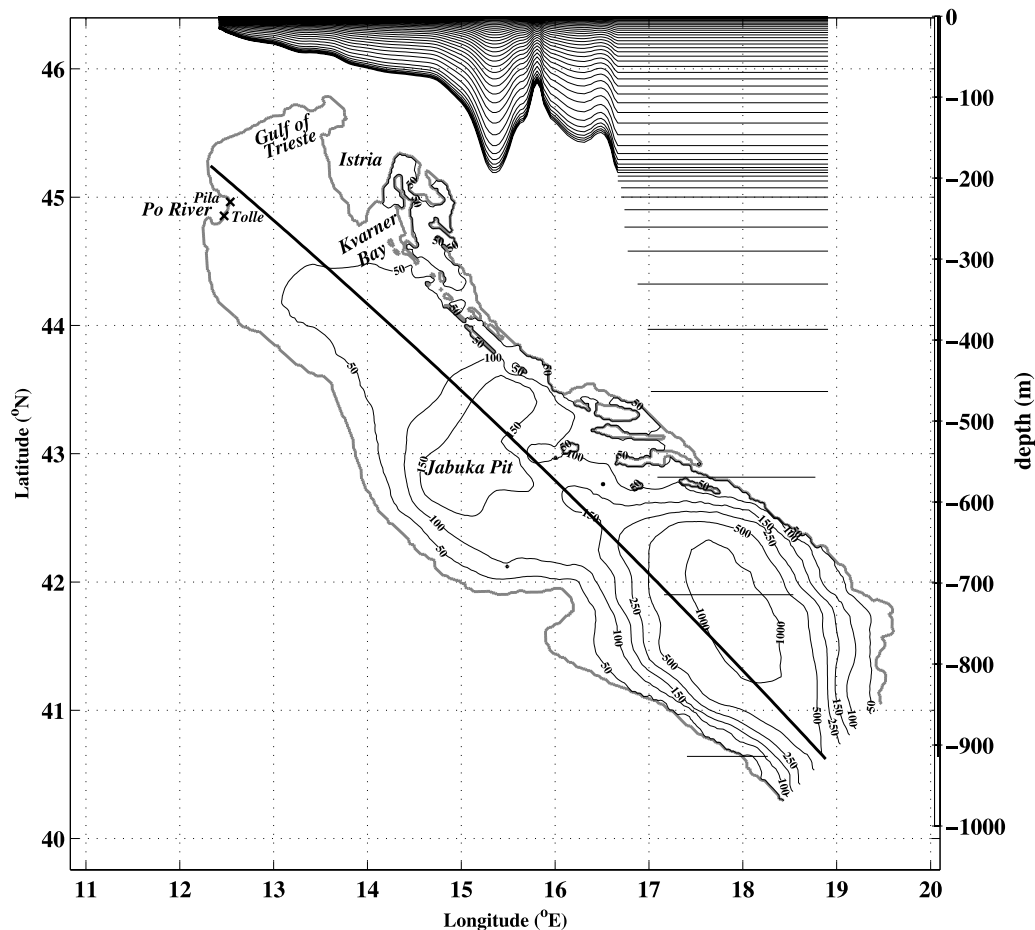
Figure 2. A section showing the vertical grid along the axis of the domain (thick black line), and associated depth scale on the right for the 2-km-resolution NCOM Adriatic Sea model. The model uses 36 sigma levels over 14 z levels. The vertical grid transitions to z levels at 190 m depth. Bathymetry is contoured in meters on the map.

nonhydrostatic and uses parameterization schemes for subgrid-scale convection, shortwave and longwave radiation processes, and mixed-phase cloud microphysics. The COAMPS system is run in reanalysis mode and contains a three-dimensional multivariate optimum interpolation (MVOI) analysis technique to generate the initial conditions for the COAMPS model in each data assimilation cycle. In this step, quality-controlled data from radiosondes, aircraft, satellites, and surface observations are used to create an MVOI of winds and pressure heights, while a univariate OI is performed for temperature and moisture.

[13] Hourly COAMPS momentum fluxes as well as surface atmospheric pressure are used to drive NCOM. Thermal surface forcing for NCOM consists of COAMPS longwave radiation and latent and sensible heat fluxes computed from hourly COAMPS wind speed, air temperature, humidity, and NCOM sea surface temperature using the bulk formulas of *Kondo* [1975], as described by *Martin and Hodur* [2003]. Evaporation derived from the latent heat flux, along with COAMPS precipitation, is used to form the moisture flux for the surface salt flux calculation. In addition, penetrating COAMPS solar radiation modifies the ocean temperature.

[14] A 27-km-resolution COAMPS atmospheric model reanalysis on a grid of dimensions 193 × 97 × 30 levels

covering the Mediterranean Sea area was used to drive a 6-km-resolution NCOM ocean model (of grid size 576 × 288 × 40 levels, 15 of which were sigma levels) of the entire Mediterranean Sea. The atmospheric fields produced were part of 12-hour incremental data assimilation cycles (with 24-hour forecasts) over the time period of interest. Further details and an evaluation of the system were documented by *Hodur et al.* [2001]. The Mediterranean Sea model was spun-up for 4 years (through June 2001). Observed monthly averaged climatological river runoff values were specified for the 54 major rivers flowing into the Mediterranean Sea based on the database developed by *Perry et al.* [1996].

[15] The Mediterranean Sea model state valid 1 January 2001, 1200 UT was used to initialize the 2-km-resolution nested model whose domain covers the Adriatic Sea. A 6-month Mediterranean forecast run was then used to supply lateral boundary conditions for the 2-km-resolution model. Boundary fields were updated at a 12-hour frequency and interpolated linearly in time in between. The Orlanski radiation condition was used for temperature, salinity, and normal velocity, while the Flather condition was used for elevation, and a zero-gradient condition was used for tangential velocity [*Rochford and Martin*, 2001]. The lateral boundary is located at the entrance to the Adriatic Sea
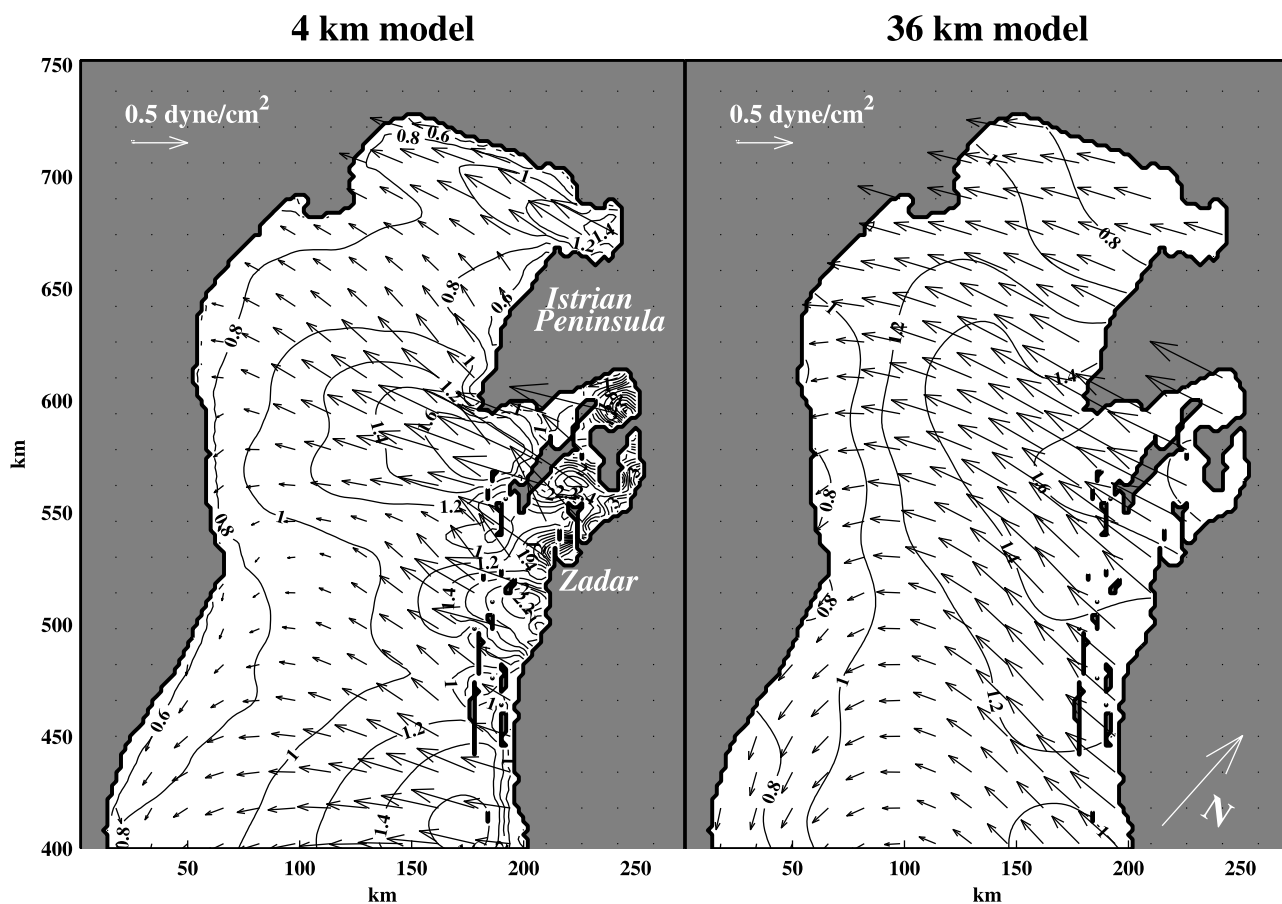
Figure 3. COAMPS wind stress statistics for 28 January to 4 June 2001 on (left) the inner 4-km-resolution nest and (right) the outer 36-km-resolution nest over the northern Adriatic. The mean is represented with arrows, while the RMS vector amplitude is contoured at an interval of 0.2 dyne/cm². Fields have been interpolated to the 2-km ocean model grid, and every eighth arrow is featured.

(Strait of Otranto) and is thus far removed from the locus of interest of these simulations. No adverse circulation effects were observed in the northern Adriatic due to the open boundary treatment.

[16] In the Adriatic simulations, a set of surface flux fields from the inner 4-km nest of a triply nested COAMPS atmospheric model reanalysis centered over the Adriatic Sea (Figure 1) was used to force the NCOM high-resolution ocean nest for a simulation from 1 January to 6 June 2001. The atmospheric fields in the COAMPS Adriatic atmospheric model reanalysis were generated using 12-hour incremental data assimilation cycles with 15-hour forecasts. The COAMPS model was run with three nested grids that are one-way interactive. The nests were integrated simultaneously, with lateral boundary conditions at the nest interfaces provided every time step. To explore the impact of the resolution of the forcing on the ocean model, the 2-km-resolution NCOM Adriatic simulation was repeated using atmospheric forcing fields taken from the outermost nest (36 km) of the COAMPS Adriatic simulation.

[17] The topographic data for the COAMPS atmospheric model are based on the U.S. Defense Mapping Agency's 100-m-resolution data set. The 100-m-resolution data set was interpolated to a 1-km-resolution grid, which then was interpolated to the model grid meshes. The Mediterranean Sea bathymetry used by the 6-km-resolution NCOM ocean

model was constructed from smoothing the 1/60° resolution U.S. Navy Digital Bathymetric Database (DBDB1). The Adriatic Sea bathymetry was digitized from Navy charts of depth soundings and then gridded onto a high-resolution finite-element mesh [*Cushman-Roisin and Naimie*, 2002]. It was subsequently interpolated to the 2-km-resolution NCOM ocean model grid and matched to the Mediterranean bathymetry near the open boundary.

[18] The Adriatic Sea ocean model has 50 vertical levels (36 of which are sigma levels) and 136×376 horizontal grid cells. Highest resolution is achieved in the surface and bottom boundary layers (Figure 2). The vertical grid affords enhanced resolution in the shallow northern Adriatic waters using terrain-following (sigma) coordinates. Pressure gradient errors associated with sigma levels [*Mellor et al.*, 1994] are avoided in the deeper southern Adriatic by employing z levels in areas of steeply sloping bathymetry.

3. Characterization of Atmospheric and Hydrological Forcing

[19] The northern Adriatic atmospheric circulation is dominated by a wind pattern termed "bora" whereby the mountains of eastern Italy, Slovenia, and Croatia accelerate fast, cold winds across the Adriatic Sea [*Smith*, 1987]. The bora, as represented in the wind stress statistics from
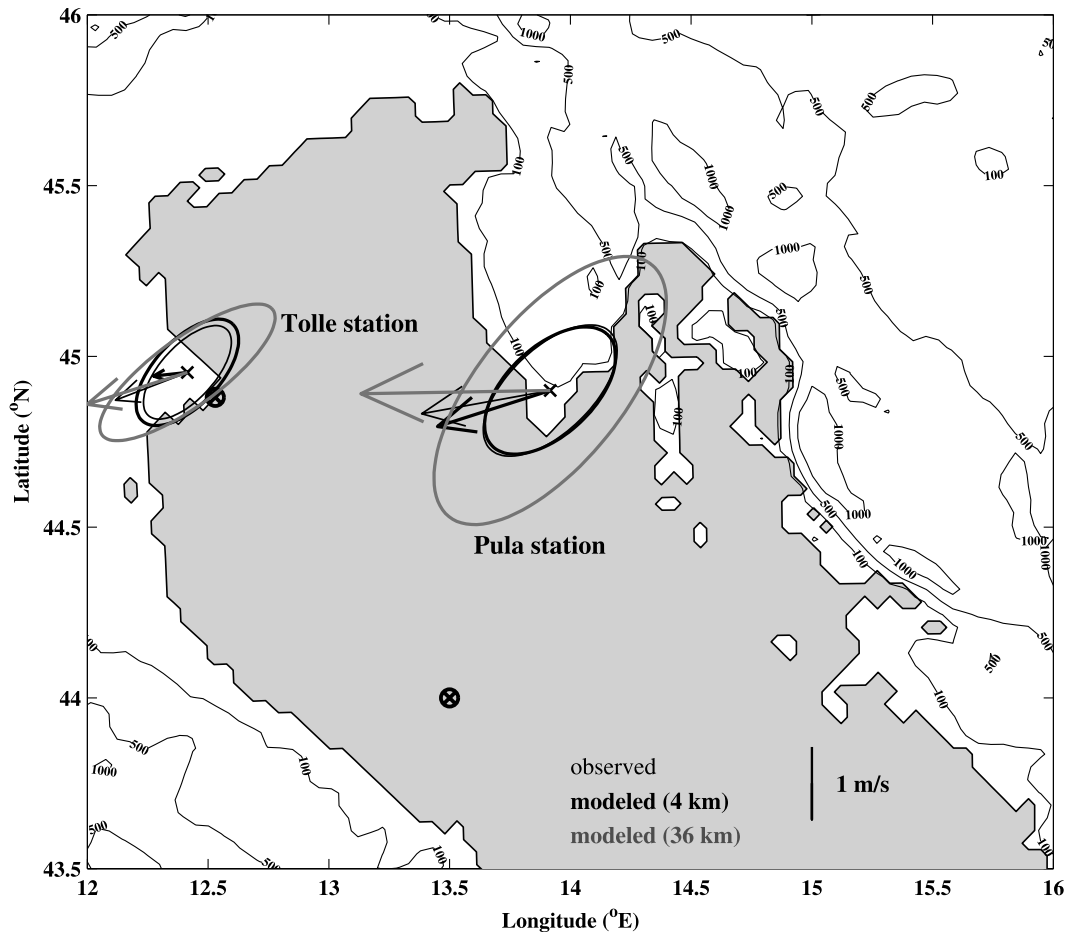
Figure 4. Mean (arrows) and principal ellipses of standard deviation (ovals) for observed and modeled 10-m wind velocities at the Tolle and Pula stations. Statistics were computed for 28 January to 4 June 2001. Locations of ADCP ocean observations are marked with a circled cross. Land topography is contoured in meters.

28 January to 4 June 2001 in the COAMPS 4-km-resolution model (Figure 3), consists of several spatially distinct prongs of northeasterly winds that are strongest on either side of the Istrian peninsula. Maximum mean wind stress is located over the Gulf of Trieste, Kvarner Bay, and offshore of Zadar. The 36-km COAMPS mean wind stress fails to resolve the bora fingers situated over the Gulf of Trieste and off Zadar. Where the bora blows over the ocean, the amplitude of the mean wind stress is typically one third to one half the amplitude of the fluctuations in each model. In general, mean and fluctuating wind stress have larger amplitudes in the 36-km-resolution model and follow a more diffuse pattern over much of the eastern Adriatic. However, in the Gulf of Trieste and offshore of Zadar, fluctuating and mean wind stress values are stronger in the 4-km-resolution model. Also, in some nearshore regions, elevated fluctuations exist in the 4-km-resolution simulation, presumably reflecting the capability of the higher-

Table 1. Comparison of Observed and Modeled Wind Velocity Statistics[a]

	Magnitude of Mean	Orientation of Mean	Standard Deviation of Principal Component	Orientation of Major Axis	Magnitude of Error of Mean Vector	RMS Error
			Pula			
Observed	1.80	−100.24	2.32	45.90		
Modeled (4 km)	1.63	−107.66	2.21	46.58	0.28	1.20
Modeled (36 km)	2.61	−90.96	4.47	38.81	0.88	2.63
			Tolle			
Observed	1.07	−111.15	1.61	42.28		
Modeled (4 km)	0.47	−96.31	1.83	43.17	0.62	1.10
Modeled (36 km)	1.46	−107.67	2.92	53.73	0.40	1.66

[a]Due north is 0° in the reported orientations, and negative angles are counterclockwise from north. Units are in meters per second. The magnitude of the error of the mean vector is the magnitude of the difference between the observed and modeled mean vectors. In the computation of RMS error, the time series were projected into the respective major axis orientations given in the table.
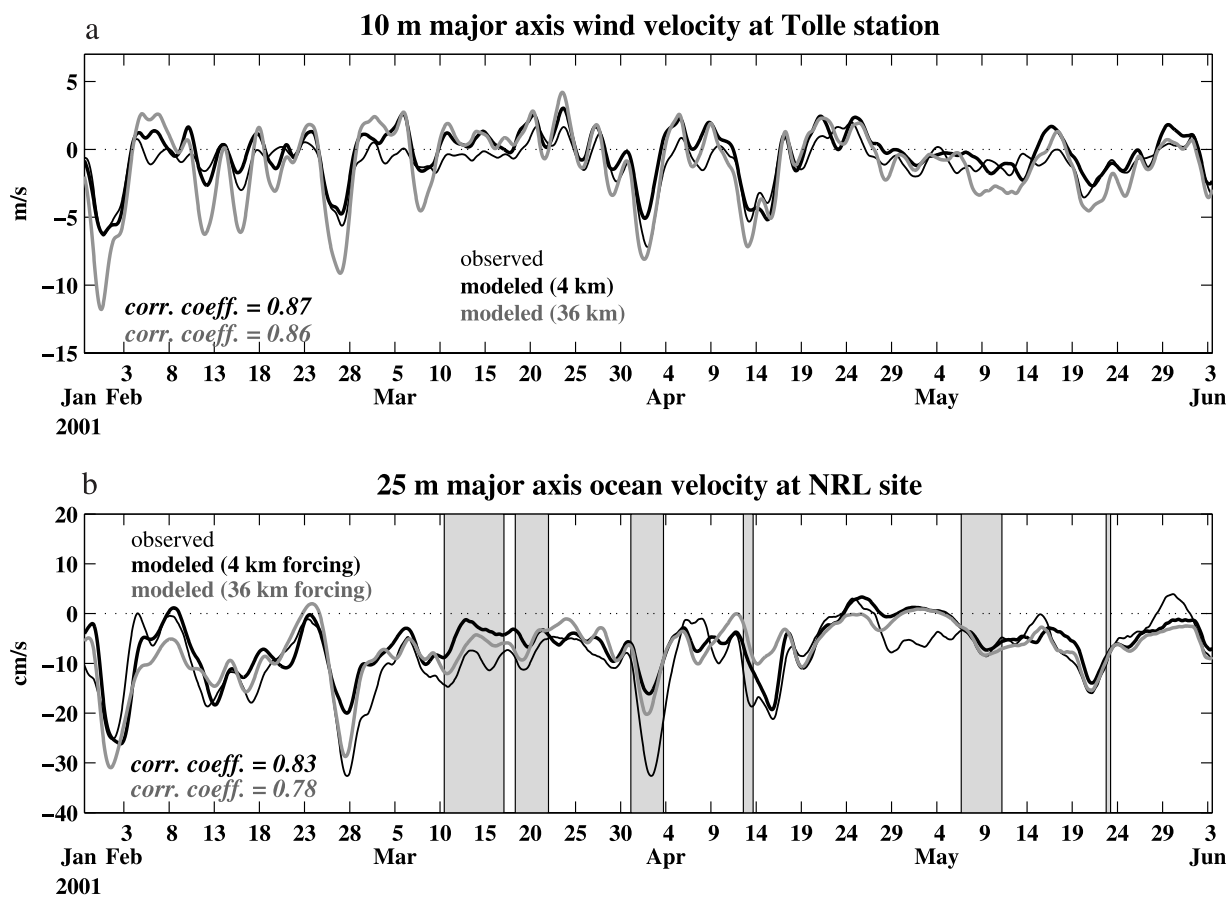
Figure 5. Time series of observed and modeled (a) 10-m major axis wind velocity at the Tolle station and (b) 25-m major axis ocean velocity at the NRL site for 28 January to 4 June 2001. The time series have been projected into the respective major axis orientations given in Tables 1 and 2. Correlation coefficients are given in the figure for the 4-km model/forcing relative to observations (black) and the 36-km model/forcing relative to observations (shaded). Times when the Po River discharge exceeds 3000 m^3/s are shaded in gray in Figure 5b.

resolution model to produce coastal circulations such as the sea breeze, land breeze, and local enhancements due to flow around coastal features.

[20] A comparison of COAMPS 4-km-resolution wind velocity with data collected during an observational plane flight along the axis of the northern Adriatic as part of the Mesoscale Alpine Project field campaign in 1999 [*Bougeault et al.*, 2001] verifies that the velocity structure of the bora is captured exceedingly well in terms of shape and magnitude by the 4-km-resolution COAMPS model. *Signell et al.* [2003] compared 4-km-resolution COAMPS and other meteorological model wind fields against observed winds over the northern Adriatic Sea at an ocean site near Venice for a 2-month period in spring 2001. The evaluation of model wind velocity values over 125 days using observations at two land locations is presented in section 4. The vast difference in the wind stress patterns generated over the ocean by the 4- and 36-km-resolution models points to the difficulty of evaluating high-resolution models over extended domains in data-scarce regions. This topic will be addressed in section 7.

[21] The 2-km-resolution Adriatic Sea model is forced by observed daily river discharge values of the Po River measured at the Pontelagoscuro gauge with salinity set to 0 psu and discharge temperature set to monthly climatological values. On the basis of historical [*Nelson*, 1970] and recent observations from December 2000 and June 2001 (A. Ogston, personal communication) the total Po River discharge is divided in the model between the Pila (80%) and Tolle (20%) river branches on the Po delta (see Figure 2). River runoff is injected into the top sigma level following the method of *Kourafalou et al.* [1996]. The Po River experienced six discharge events in excess of 3000 m^3/s during 28 January-4 June 2001. March 2001 contained two events separated by about a day where the runoff exceeded this threshold continuously for over 3 days.

[22] As shown in section 5, it is important to represent the Po River discharge in the ocean model, as one of the ADCP sites is located near the mouth of the Po. However, the effects of river discharge on ocean circulation features are not investigated directly here.

4. Comparison With Atmosphere Observations

[23] COAMPS 10-m wind velocities from the 4- and 36-km-resolution models are compared with wind velocities
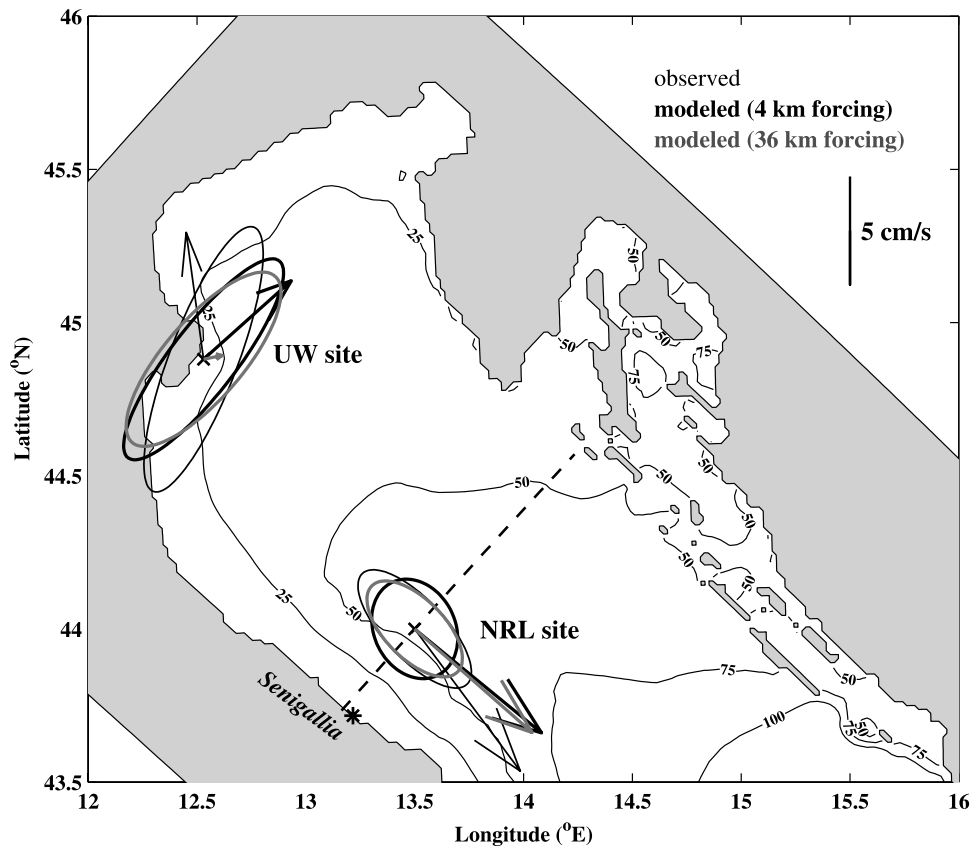
Figure 6. Mean (arrows) and principal ellipses of standard deviation (ovals) for observed and modeled 5-m ocean velocities at the UW and NRL sites. Statistics were computed for 28 January to 4 June 2001. Bathymetry is contoured in meters. The dashed line shows the Senigallia transect.

taken at meteorological stations at Pula, Croatia, and at Tolle, Italy (near where the Po River discharges into the Adriatic). All observed and modeled values are recorded or interpolated hourly and subsequently filtered with a low-pass Butterworth filter with 21-hour cutoff. Velocities are rotated into the principal axis orientations to isolate the major direction of variability.

[24] At the Pula station the magnitude and direction of the mean velocity produced by the 4-km-resolution model is in better agreement with the observation than the same quantities from the 36-km-resolution model (Figure 4 and Table 1). The standard deviation of the principal component of wind velocity from the 36-km-resolution model is twice that of the observation and of the 4-km-resolution model.

[25] At the Tolle site the mean velocity of the 36-km-resolution model is larger than that of the observed or 4-km-resolution model but is closer in magnitude and direction to the observations than is the 4-km-resolution model. As at the Pula station, the standard deviation of the principal component of the 36-km-resolution model wind velocity is larger than that of both the 4-km-resolution model and the observation.

[26] At both sites, the standard deviation of the principal component is within 0.22 m/s of the observed values for the 4-km model, and within 2.15 m/s of the observed values for the 36-km model. Both models reproduce the orientations of the observed major axis; although the orientations of the 4-km model major axis accord somewhat

better with the observed major axis orientations at both stations. The RMS errors of the 4-km model are smaller than the RMS errors of the 36-km model at the Pula and Tolle stations. Furthermore, only the 4-km model RMS errors are smaller than the observed and modeled standard deviation at both sites.

[27] The correlation coefficients of the 4- and 36-km-resolution model velocities relative to the observations at the Pula station are 0.87 and 0.89, respectively. The correlation coefficients of the 4- and 36-km-resolution model velocities relative to the observations at the Tolle station are 0.87 and 0.86, respectively (Figure 5). Thus the modeled/observed correlation coefficients at both sites are comparable for the two different model resolutions and exceed 0.85. The observed (4-km model/36-km model) maximum lagged correlation between the Pula and Tolle stations is 0.86 (0.87/0.94).

5. Comparison With Ocean Observations

[28] As part of the EuroSTRATAFORM experiment, the University of Washington (UW) set out a tripod-mounted RD Instruments workhorse ADCP off the Po River delta near the 12-m isobath (12.53°E, 44.88°N). In an unrelated observational effort, NRL placed a trawl-resistant, bottom-mounted ADCP in the western Adriatic just off the town of Senigallia on the 57-m isobath (13.45°E, 43.91°N). *Book et al.* [2003] present an analysis of these ADCP data at the

Table 2. Comparison of Observed and Modeled Ocean Velocity Statistics[a]

	Magnitude of Mean	Orientation of Mean	Standard Deviation of Principal Component	Orientation of Major Axis	Magnitude of Error of Mean Vector	RMS Error
			UW 5 m			
Observed	5.92	−7.79	13.05	20.77		
Model, 4-km forcing	5.42	48.07	11.44	37.35	5.33	13.53
Model, 36-km forcing	0.87	78.22	10.10	40.43	5.92	10.73
			NRL 5 m			
Observed	8.16	143.53	7.02	136.84		
Model, 4-km forcing	7.55	129.48	4.77	154.12	2.02	6.11
Model, 36-km forcing	7.21	131.59	5.59	135.46	1.86	5.59
			NRL 25 m			
Observed	8.88	141.29	7.08	138.35		
Model, 4-km forcing	6.71	128.44	5.59	126.94	2.77	4.90
Model, 36-km forcing	7.71	128.06	6.18	124.35	2.23	4.72

[a]As in Table 1, but units are in centimeters per second.

NRL site. The UW and NRL sites were separated by approximately 125 km (Figure 6). The time period of overlap of these observations was 28 January-4 June 2001 (125 days).

[29] All observed and modeled values were recorded or interpolated hourly and subsequently filtered with a low-pass Butterworth filter with 21-hour cutoff. Velocities are rotated into the principal axis orientations in order to effectively isolate the alongshore (major axis/principal component) and across-shore (minor axis) directions in this region of variable coastline orientation. The 5-m UW velocity represents an average of five bins of 0.2-m spacing centered at 4.97 m depth. The uppermost NRL ADCP bin (4.6 m depth) was deemed excessively contaminated by bad data in the work of *Book et al.* [2003]. Hence the 5-m NRL velocity used here is the second bin (6.6 m depth).

[30] Neither model captures properly the orientation of the mean 5-m current at the UW site (Figure 6 and Table 2). The UW site is located in the vicinity of strongly varying coastline orientation, which may increase the model sensitivity to the exact observation position. In addition, the currents at the UW site near the mouth of the Po River are heavily influenced by shifts in the plume location, which likely lead to enhanced variability and reduced predictability. As a consequence, the UW observed standard deviation of the principal component of velocity is approximately twice the mean velocity at 5 m below the sea surface. This relationship is reproduced in the ocean model forced by the 4-km-resolution COAMPS fields but not by the model subjected to the coarser-resolution forcing.

[31] At the NRL site, the 5- and 25-m standard deviations of the principal component are of approximately the same magnitude as the mean for the observed and modeled velocities, although the 36-km forced model matches the observed values better. *Poulain* [2001] previously documented fluctuating and mean currents of comparable size along the west coast of the Adriatic in an analysis of drifter observations. Additionally, at the NRL site the mean current is aligned closely with the major axis orientation in the observed and modeled fields.

[32] The magnitude of the error of the mean vector is smallest in the 36-km forced model at the NRL site (both depths), and the RMS errors are smallest for the 36-km forced model at both sites and depths. The observed (4-km

forced model/36-km forced model) maximum lagged correlation between UW 5-m and NRL 5-m major axis velocities is 0.18 (0.32/0.51). The observed (4-km forced model/36-km forced model) maximum lagged correlation between NRL 5-m and NRL 25-m major axis velocities is 0.83 (0.55/0.85). Therefore the ocean model forced by the coarser-resolution meteorological model generates currents that are more correlated horizontally and vertically than either the observed or modeled currents using the 4-km forcing. A similar result was found in the atmosphere where wind correlations between the two meteorological stations were greatest for the 36-km-resolution model. The difference in oceanic spatial correlations generated by the two forcing resolutions will be further quantified in terms of major axis decorrelation length scales in section 6.

[33] At 25 m depth at the NRL site, surges of the current down the coast are associated with bora events (negative excursions in the time series in Figure 5). Except during April, large Po River discharge events (shaded gray) are decoupled from the bora winds and associated ocean response. The correlation coefficient of modeled currents with observed currents is greatest for the 4-km forced ocean model. The 36-km forced and 4-km forced modeled/observed correlations are distinguishable from each other with 99% confidence.

[34] Statistics were computed throughout the water column at the NRL site for currents rotated into the depth-averaged major axis orientations given in Table 3 (Figure 7). The structure of the observed mean and standard deviation of the principal component of velocity at the NRL site reveals the current to be primarily barotropic, as documented by *Book et al.* [2003] for a shorter data record

Table 3. Comparison of Observed and Modeled Depth-Averaged Ocean Velocity Statistics[a]

	Magnitude of Mean	Standard Deviation of Principal Component	Orientation of Major Axis
	NRL Depth-Averaged Velocity		
Observed	8.99	6.80	135.70
Modeled, 4 km forcing	6.91	4.94	125.97
Modeled, 36 km forcing	8.13	5.71	122.30

[a]Due north is 0° in the reported orientations and negative angles are counterclockwise from north. Units are in centimeters per second.
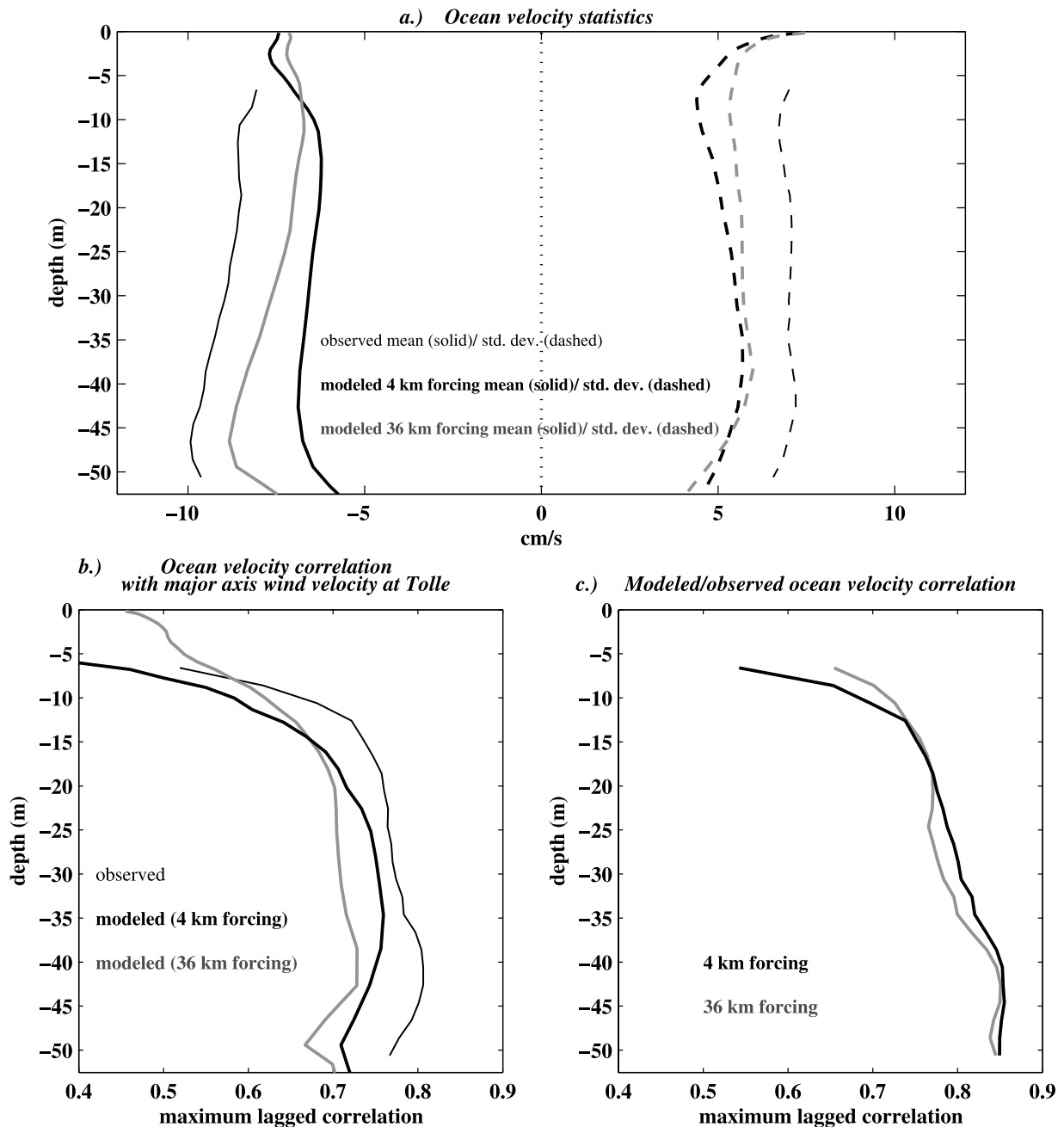
Figure 7. Modeled and observed statistics through the water column at the NRL site. All ocean velocities have been rotated into the depth-averaged principal axis orientations given in Table 3. (a) Mean (solid line) and standard deviation (dashed line). (b) Maximum lagged correlation of currents at the NRL site with major axis winds at the Tolle station, and (c) maximum lagged correlations of modeled and observed ocean currents at the NRL site.

(January through April 2001). This feature is captured by both the 4- and 36-km forced ocean model simulations (Figure 7a). The 36-km forced ocean model yields somewhat larger mean and standard deviations, more in accordance with the observations. The depth-averaged major axis current statistics of Table 3 reinforce this result, which could be explained by the increased spatial extent of large mean and fluctuating wind stress values over the ocean in the 36-km COAMPS model (Figure 3).

[35] The vertical structure of maximum lagged correlation of the ocean current at the NRL site with wind velocity at the Tolle station shows a subsurface maximum in both observed and modeled correlations (Figure 7b). (Note that in this analysis, for consistency, modeled winds are correlated to modeled currents and observed winds are correlated to observed currents.) By contrast, observed and modeled wind/current correlations are largest near the surface at the UW site (not shown). Lags of maximum correlation are
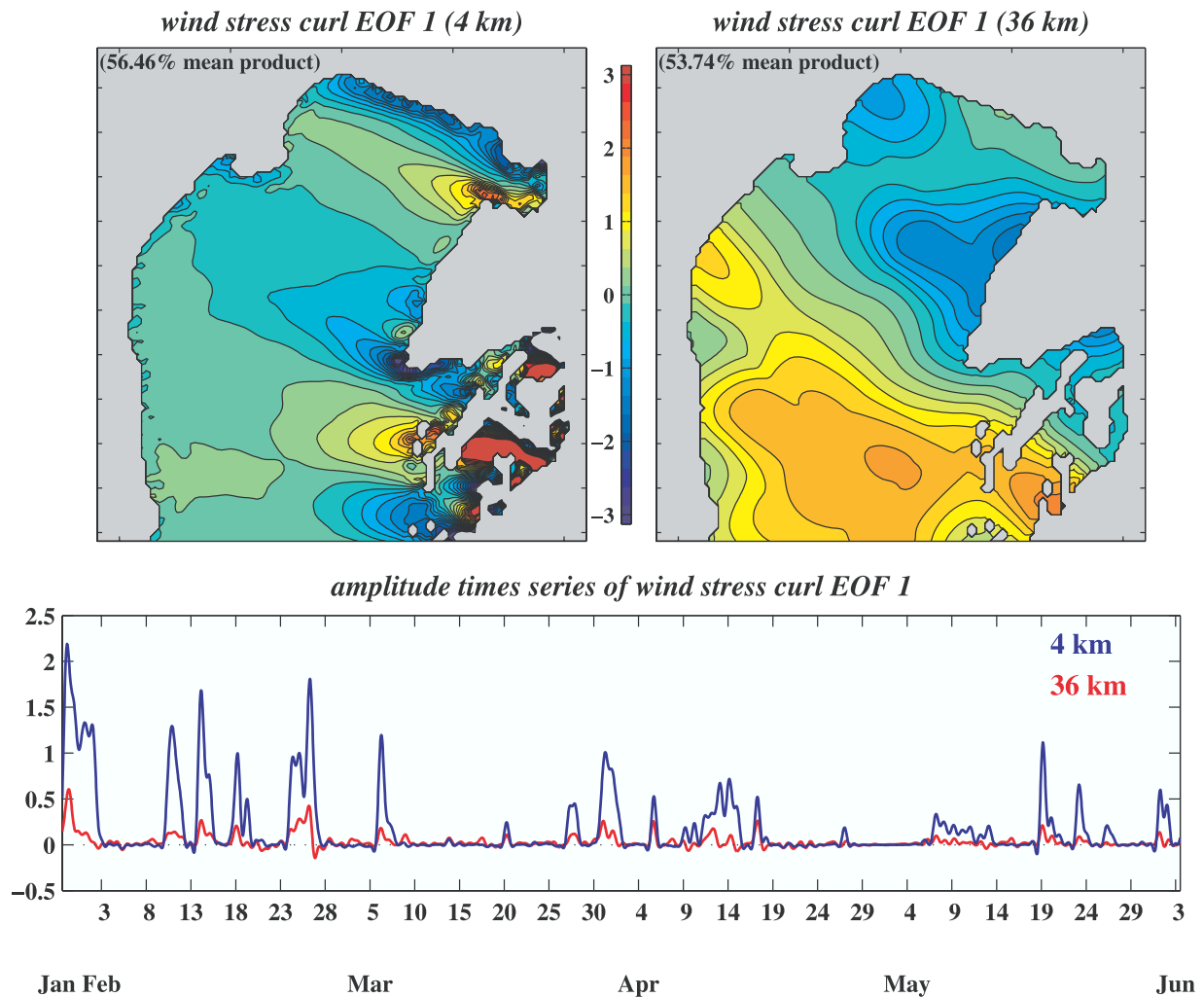
Figure 8. Wind stress curl EOF 1 and associated amplitude time series for the 4- and 36-km-resolution COAMPS simulations. The wind stress fields were interpolated to the 2-km ocean model grid prior to the computation of the curl field. The percent mean product that the EOF represents is given in the wind stress curl maps. Units of the wind stress curl are dyne/cm^3 × 10,000.

somewhat shorter in the observations compared to the models. For instance at 25 m depth the lag for observed (modeled 4-km forcing/modeled 36-km forcing) maximum correlation is 17 hours (19 hours/19 hours). The 4-km forced model better represents the depth-dependent structure and magnitude of the observed wind/current correlations compared to the 36-km forced model. However, the correlations of observed NRL currents with observed Tolle winds are larger than the correlations between modeled currents and modeled winds (for both 4- and 36-km forcing). That observed winds are more strongly correlated with observed currents at depth may be related to the observed mean and standard deviations being larger than the modeled values at this site.

[36] At the NRL site, below approximately 20 m depth, the 4-km forced model correlates better with the observed currents (Figure 7c). The correlation coefficients are distinguishable from each other with 90% confidence in the depth range of 25–37 m. This corresponds to the region of the water column where the observed and modeled fields, as shown above, were the most strongly correlated with winds at the Tolle station.

[37] Correlations at the NRL site between observed ocean currents and 4-km forced ocean currents in the upper 12 m were smaller than those of the observed ocean currents with the 36-km forced ocean currents. The 4-km forced model and 36-km forced model differ in their representation of the dynamics in the near-surface waters at the NRL site. Typically, the 36-km forced model produces a deeper mixed layer, as determined by the depth at which the temperature has an anomaly from the surface waters of more than 0.05° (not shown). This characteristic is particularly pronounced during the spring period of mid-March through April and may contribute to the discrepancy between the models in matching the observed velocity near the surface.
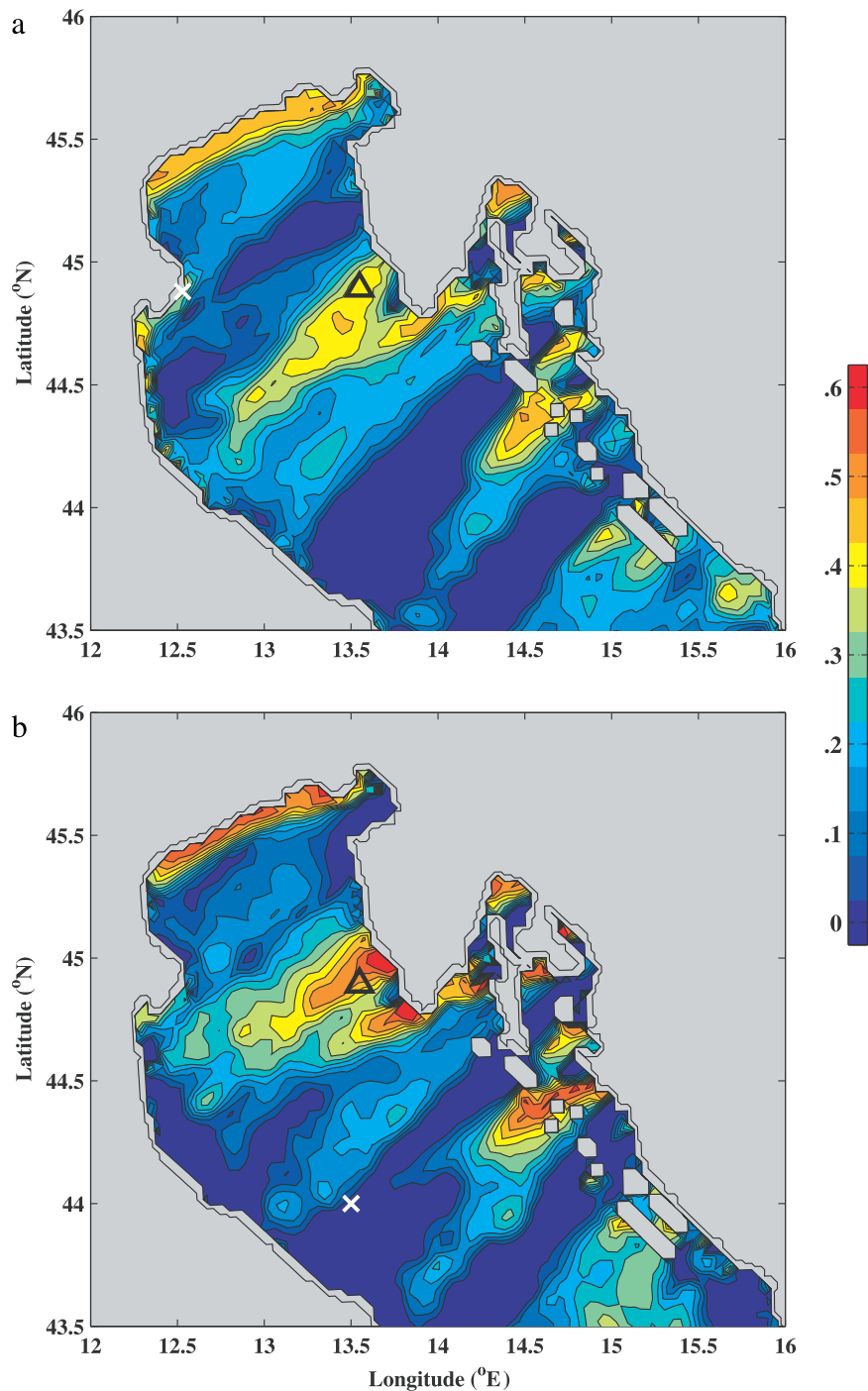
Figure 9. Maximum lagged correlation of 5-m observed major axis current at the (a) UW site and (b) NRL site with COAMPS 4-km-resolution model wind stress curl. Wind stress was interpolated to the 2-km ocean grid before calculation of wind stress curl. Lagged correlations were computed from the time series of every second wind stress curl point on the 2-km grid. The ADCP observation site being correlated with the wind stress curl is marked with a cross in each panel. Statistics are highlighted in the text for the location indicated by the triangle.

[38] *Book et al.* [2003] demonstrate the linkage between the COAMPS wind stress and the observed currents at 43 m depth at the NRL site. They found that maximum lagged correlations followed a pattern consistent with the bora imprint. To conclude this section we further quantify and extend this result.

[39] The COAMPS wind stress curl pattern generated by the 4- and 36-km-resolution models is encapsulated in the mode-1 Empirical Orthogonal Function (EOF) (Figure 8). (In these EOF analyses, the mean has been retained since it contains a strong signature of the bora.) The wind stress curl mode-1 EOF is stronger in amplitude
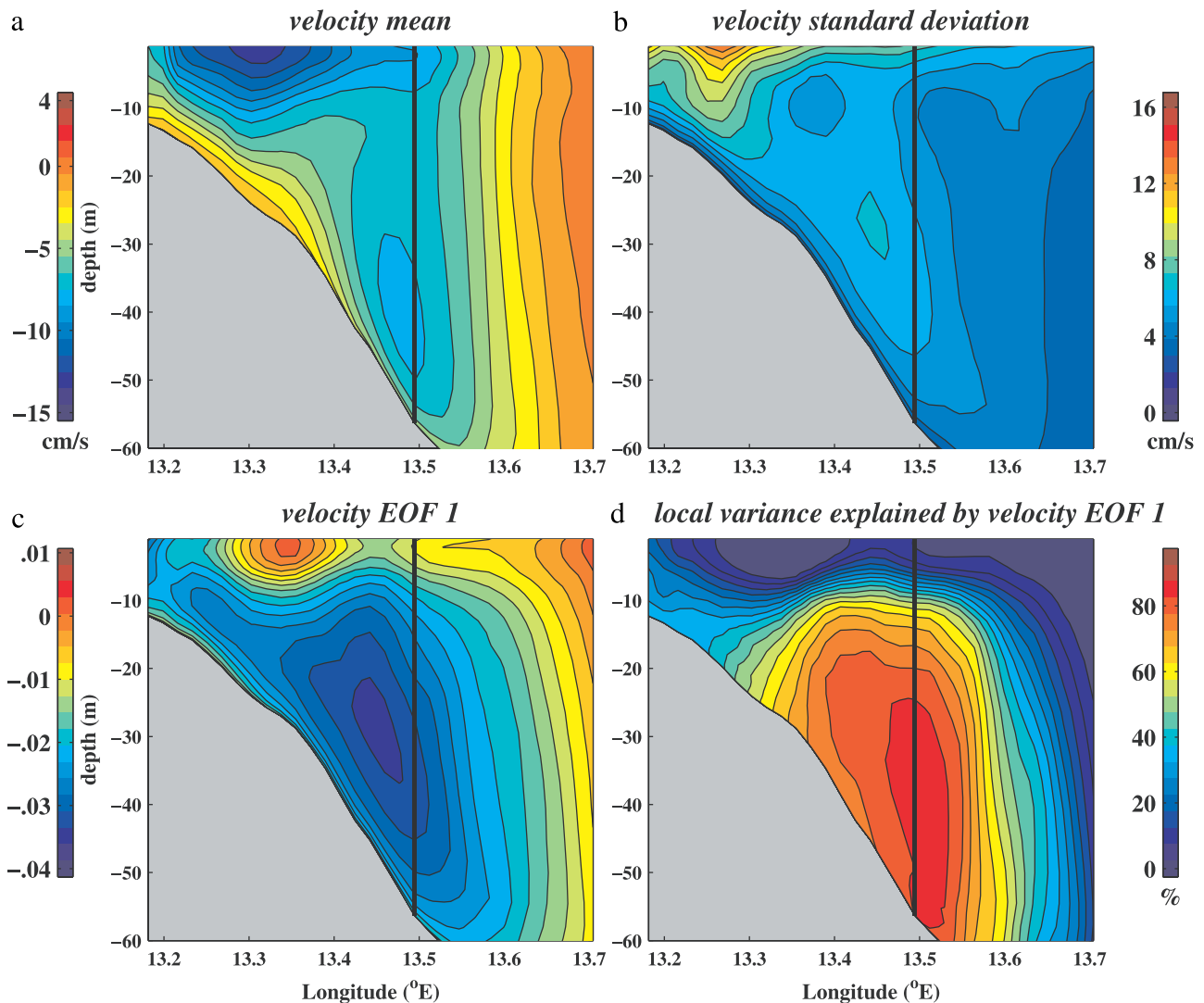
Figure 10. Statistics for velocity through the Senigallia section (dashed line in Figure 6). (a) Mean, (b) standard deviation, (c) EOF 1, and (d) local percent variance explained by EOF 1 are displayed. Velocity EOF 1 contains 42.85% of the total variance (because of the variable spacing of the sigma coordinates, the time series at each grid point was normalized by the square root of the grid cell area before the EOF calculation. The EOF is displayed unweighted above). The black vertical line indicates the location of the NRL ADCP site.

and more highly structured spatially on the 4-km-resolution grid. The fine-scale structure on the 4-km-resolution grid is evidenced by several regions of maximum negative wind stress curl located over the northern portion of the Gulf of Trieste, off the southern tip of the Istrian peninsula, and north of the Croatian town of Zadar. By contrast, the sole region of negative wind stress curl in the 36-km-resolution mode-1 EOF is weaker in magnitude and occurs over a broad swath of the far northern Adriatic. Gradients of wind stress curl are quite weak on the 36-km grid, and positive wind stress curl extends across the region below the Istrian peninsula.

[40] Though the observed 5-m currents at the UW and NRL sites are poorly correlated with each other, as documented earlier in this section, the currents at the two sites nonetheless respond to a similar wind stress curl spatial pattern represented by the 4-km COAMPS model (Figure 9). The three regions that are most highly correlated with the ocean response at the two sites correspond to areas of large horizontal shear in the bora winds, that is, large negative wind stress curl (Figures 3 and 8). The maximum correlation (lag) of the major axis 5-m current with the wind stress curl located at the triangle in Figure 9 is 0.49 (16 hours) for the NRL site and 0.44 (0 hours) for the UW site. The observed currents respond more quickly to the regions of greatest simulated wind stress curl at the UW site compared to the NRL site, with correlations being smaller for the UW site. At the NRL site, the correlations of the current with wind stress curl increase substantially at 25 m depth but reproduce the same spatial structure (not shown). To further explore the dynamical connection between the ocean and the atmosphere, section 6 will present statistical correlations
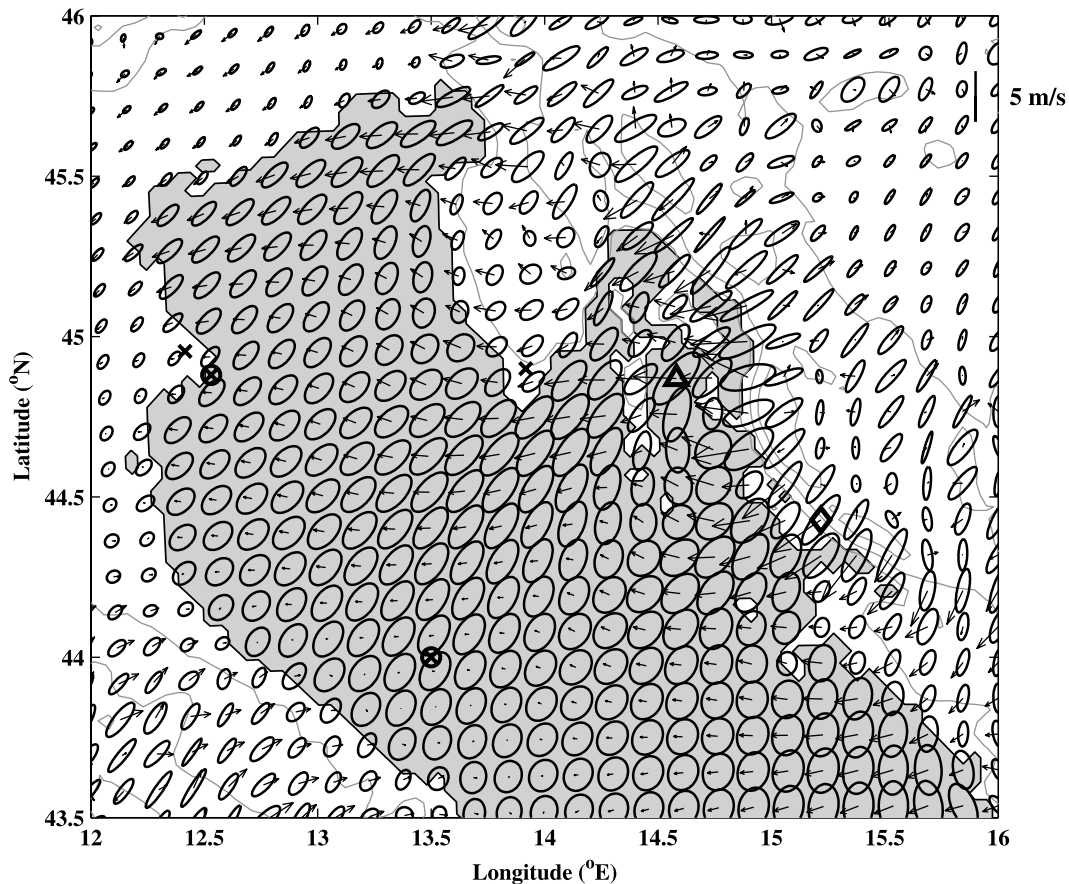
Figure 11. Mean (arrows) and principal ellipses of standard deviation (ovals) for 10-m COAMPS wind velocity from the 4-km-resolution model for 28 January to 4 June 2001. Statistics are shown for every third point on the grid. Ocean ADCP observation locations are marked with circled crosses. Atmospheric meteorological stations are indicated with crosses. The position of maximum mean magnitude of wind velocity is shown with a diamond, while the largest standard deviation of the principal component is located at the triangle. As in Figure 4, land topography is contoured at 100, 500, and 1000 m.

of this main wind stress curl pattern with the modeled ocean response.

6. Statistics and Patterns of Ocean-Atmosphere Circulation

[41] In this section, modeled oceanic and atmospheric velocity statistics for the 125-day simulations are presented on cross sections and horizontal maps. The connection between the ocean and atmosphere is quantified through EOFs and their amplitude time series correlations.

[42] The 4-km forced model velocity mean and standard deviation through the Senigallia section out to 13.7°E (section location drawn with a dashed line in Figure 6) reveal the structure of the current field in the vicinity of the 57-m isobath where the NRL ADCP was situated (black line) (Figure 10). The mean and fluctuating currents are barotropic near the NRL site, as verified in the observations, but are baroclinic inshore of the NRL site. The mean current in the upper 10 m exceeds 10 cm/s, while the standard deviation is greater than 8 cm/s. The shape of the fluctuations reflected in the standard deviation mimics a classic coastal current. The velocity mode-1 EOF is

strongly correlated with the 4-km-resolution wind stress curl mode-1 EOF of Figure 8 (maximum correlation coefficient of 0.82 lagging by 9 hours). The structure of this primary velocity EOF (accounting for 42.85% of the total variance) suggests a wind forced response that dominates the midshelf region and whose magnitude is strongest at depths exceeding 20 m. This mode explains a majority of the local variance below about 15 m depth in the waters surrounding the NRL site. The depth-dependent response to the wind forcing represented by the velocity mode-1 EOF is consistent with the observations at the NRL site where the correlation of observed currents with observed winds was greatest below about 20 m depth.

[43] Fluctuations of the surface-intensified nearshore coastal current about the mean state are represented by the velocity mode-2 EOF comprising 19.69% of the variance (not shown). Together, the first two modes account for the majority of the variance in the western portion of the Senigallia transect.

[44] The orientation of the principal axes of COAMPS 4-km-resolution wind velocity during winter and spring 2001 is quite variable over the domain (Figure 11). Preferred orientations are apparent in the mountainous regions
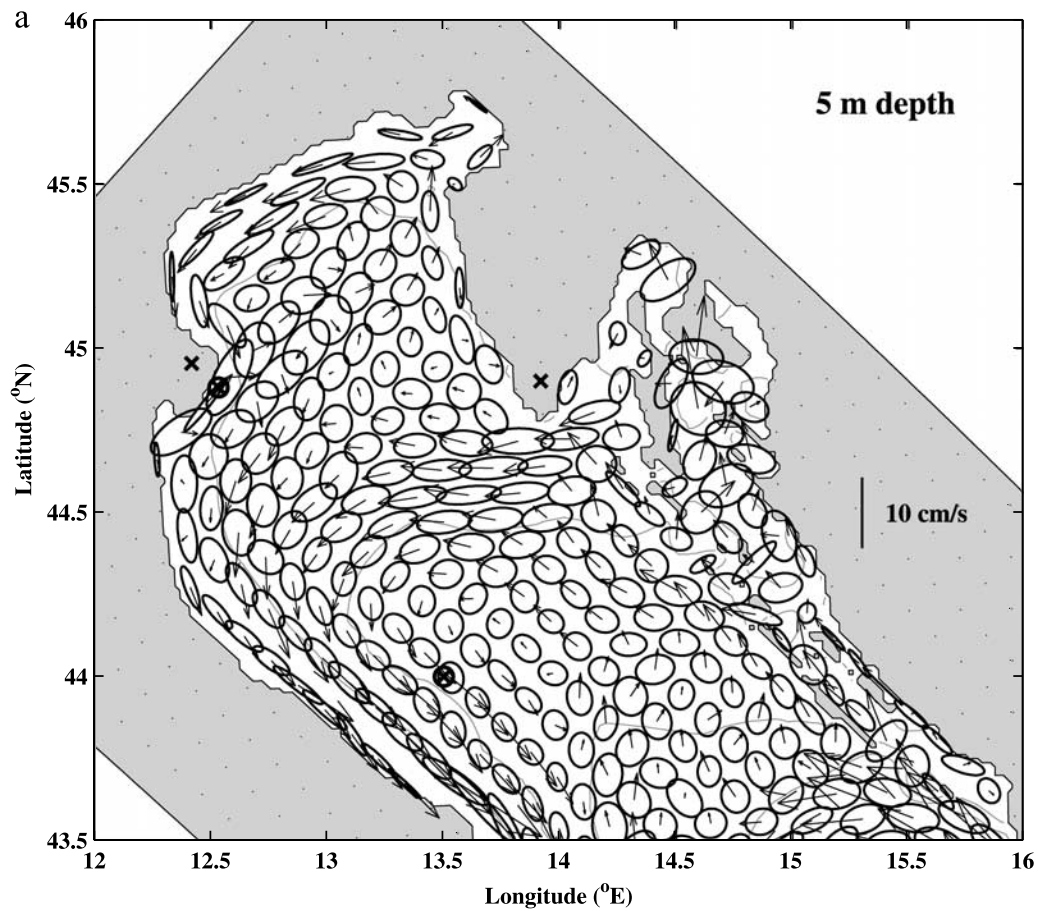
Figure 12. As in Figure 11, but for ocean model velocity (forced by the 4-km-resolution COAMPS model) at (a) 5 m and (b) 25 m depths, using a common scale. Statistics are shown for every sixth grid point and represent the period 28 January to 4 June 2001. As in Figure 6, ocean bathymetry is contoured for the 25-, 50-, 75-, and 100-m isobaths.

(e.g., where the bora has its origin). Over the ocean, the wind velocity ellipses are larger and more circular, indicating increased variability in all directions. Over the Po River drainage basin, the winds have virtually no dominant axis of variability and are extremely weak in the mean. Mean values are highest in the area of the bora (in the Slovenian and Croatian mountains and adjacent ocean) as well as in the Appenine Alps. The maximum mean wind velocity (5.76 m/s) is found at the site marked by the diamond. The maximum standard deviation of the principal component (6.54 m/s) is found at the point marked with a triangle.

[45] The 4-km forced NCOM ocean model velocity mean (arrows) and principal ellipses of standard deviation at 5 m depth during winter and spring 2001 display the anticipated polarization of coastal currents in the northern and western Adriatic (Figure 12). The current recirculates south of the Istrian peninsula and north of the Jabuka Pit. Variability is large in the area adjacent to where the Po River discharges and in the confined regions behind the Croatian Islands. These general features of the circulation match the findings based on drifter release reported by *Poulain* [2001]. At 25 m depth the magnitudes of the mean and standard deviation are reduced. Except for the pronounced circulation along the

northern coast, many of the same circulation features as were evident at 5 m depth are apparent at 25 m depth. In addition, southward flow along the Istrian peninsula is a prominent feature at this depth.

[46] The ocean velocity mode-1 EOFs at 5 m depth generated by the 4- and 36-km forced models are quite different in the far northern Adriatic (Figure 13). The cyclonic circulation that monopolizes the shallow northern Adriatic in the 4-km forced model is not well formed in the 36-km forced model. The anticyclonic circulation cell off the Istrian peninsula is absent in the 36-km forced model. Instead, the recirculation to the south of the Istrian peninsula extends farther north in the 36-km forced model than it does in the 4-km forced model.

[47] At 25 m depth, the anticyclone apparent in the velocity mode-1 EOF is strengthened on the 4-km grid. The circulation of the velocity mode-1 EOF of the 36-km forced model is quite weak in the far northern Adriatic (the magnitude of the currents is supplied by the amplitude time series, shown in the bottom panel of Figure 13). The features of the circulation from the 4-km forced model, just highlighted, locally account for a substantial fraction of the mean product, with the southward flow along the Istrian
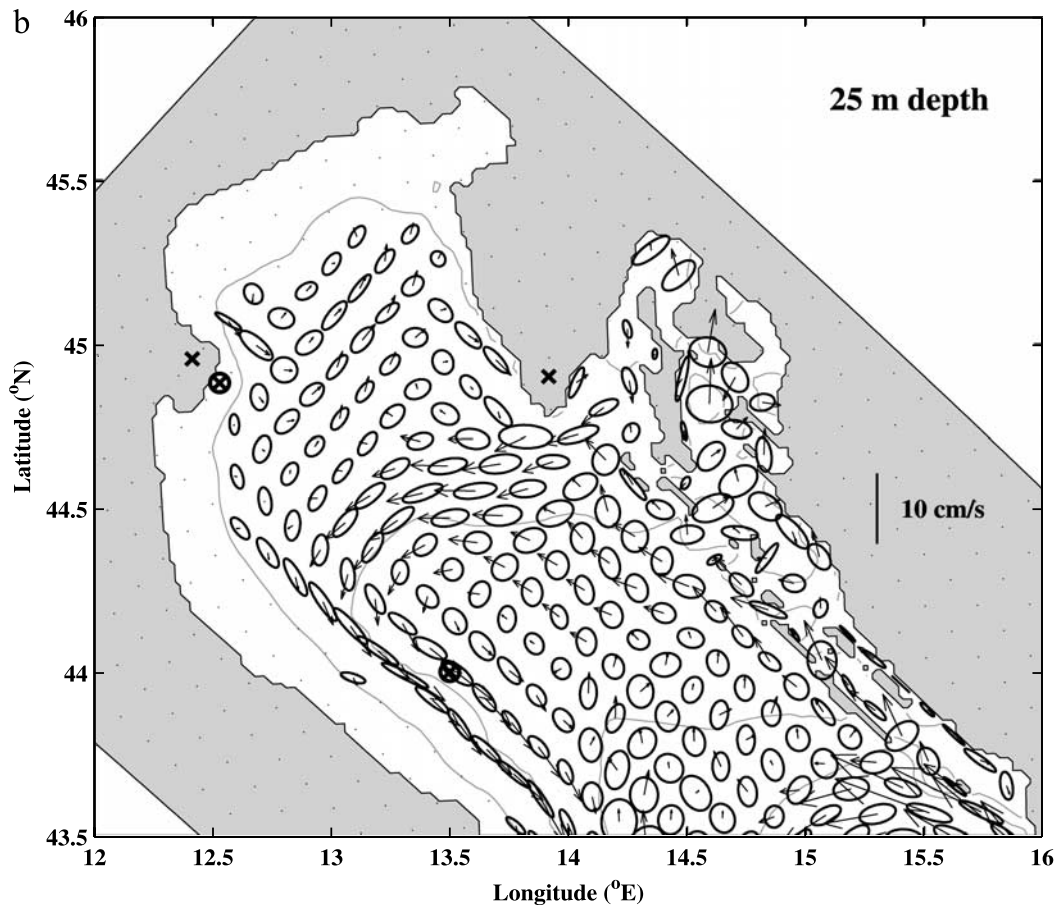
Figure 12. (continued)

peninsula increasing in importance with depth (Figure 14). The double-circulation cell that is a generic feature of the circulation in the model forced by the 4-km-resolution atmospheric fields was produced by a model forced for several days by realistic bora winds [*Paklar et al.*, 2001] and has been partially observed in the field, as noted in section 1.

[48] The mode-1 EOF wind stress curl patterns (Figure 8) are highly correlated with the ocean model velocity mode-1 EOF patterns of Figure 13 (Table 4). The correlation coefficients increase with depth for both the 4- and 36-km forced ocean simulations. The lag of the maximum correlation also increases slightly with depth. An increase with depth of correlation with wind at the NRL site in both the observations and models was presented in section 5. This feature observed at a single point is shown in the model simulations to apply to a broader region of the northern Adriatic, where waters are deeper than 25 m.
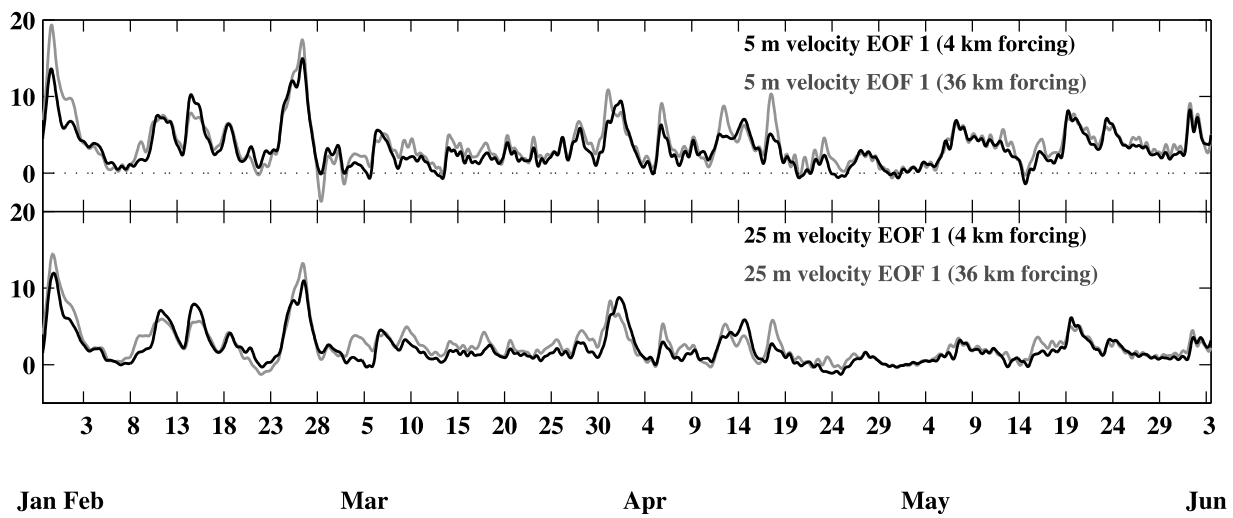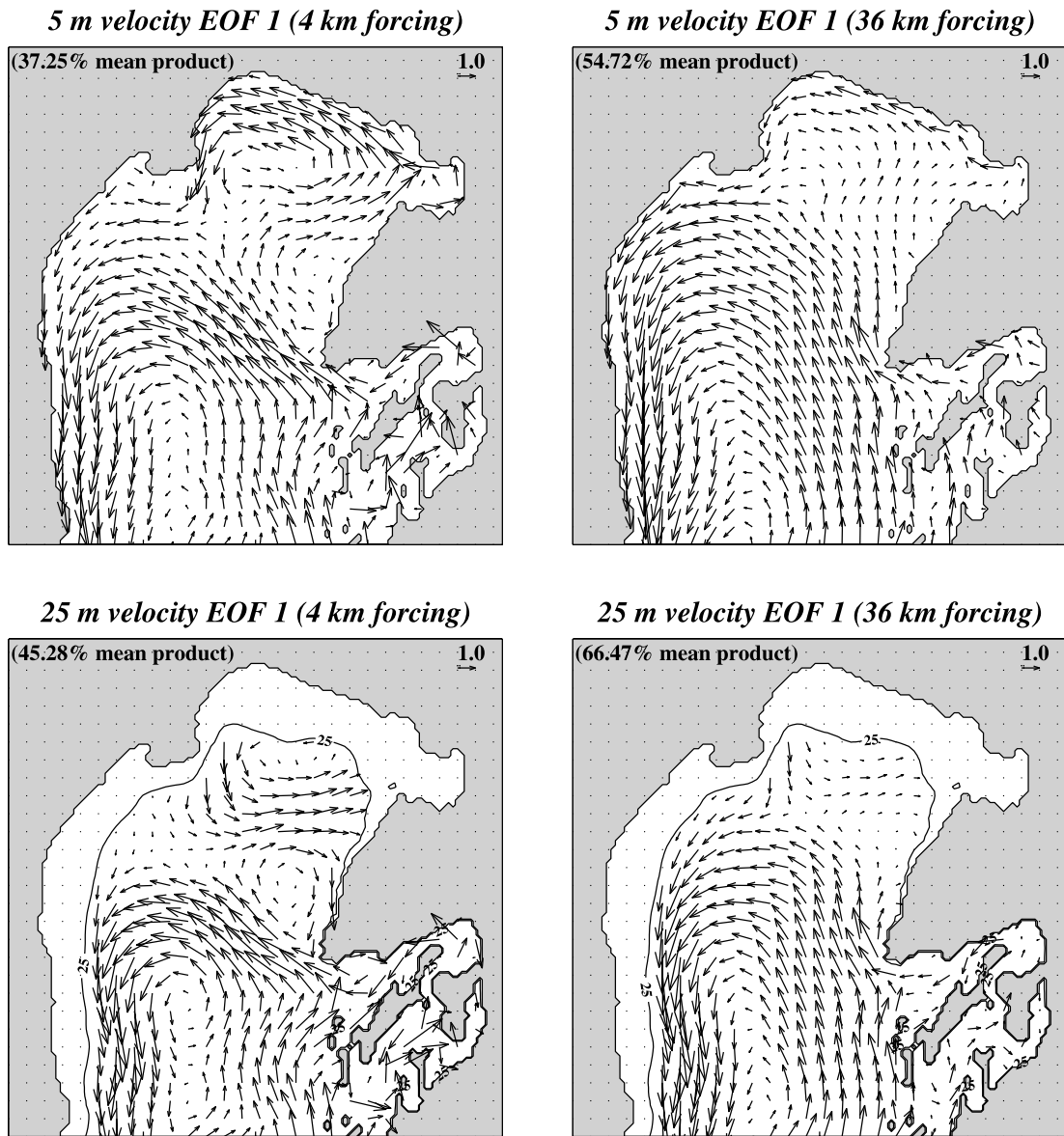
[49] An additional manner in which the resolution of the wind forcing leaves its mark on the ocean is through spatial correlation scales. Maximum lagged cross correlations between the modeled 25-m major axis velocity at the NRL site and the modeled major axis velocity elsewhere using 4- and 36-km-resolution forcing (Figure 15) provide a measure of the major axis decorrelation length scale. The major axis decorrelation length scales generated by the 4-km forcing are shorter than those obtained with the model using the

36-km forcing, as indicated by the extent of the 0.9 contour. A similar result was obtained for major axis velocities at 5 m depth (not shown). Elevated correlations between the modeled velocity at the NRL site and the modeled velocity off the Istrian peninsula occur with 4-km forcing but not with 36-km forcing. A linkage between these two regions of the basin was hypothesized by *Book et al.* [2003] and appears to be substantiated here.

7. Discussion and Conclusions

[50] This work was designed to evaluate ocean and atmosphere simulations of the northern Adriatic and to identify model-derived patterns of circulation in the ocean and atmosphere. An additional goal was to clarify and quantify the impact of the atmospheric model resolution on the winds and associated wind-driven ocean response. The 4-km-resolution (innermost COAMPS nest) atmospheric model produced clearly delineated bora fingers that were more diffuse and/or absent in the 36-km-resolution (outermost COAMPS nest) model.

[51] At two meteorological stations, the orientations of the principal ellipses of standard deviation of 10-m velocity of both models closely match the observed orientations. The standard deviations of the 36-km model principal component exceed the observed values and 4-km model values at both sites. At both stations the 4-km model produced
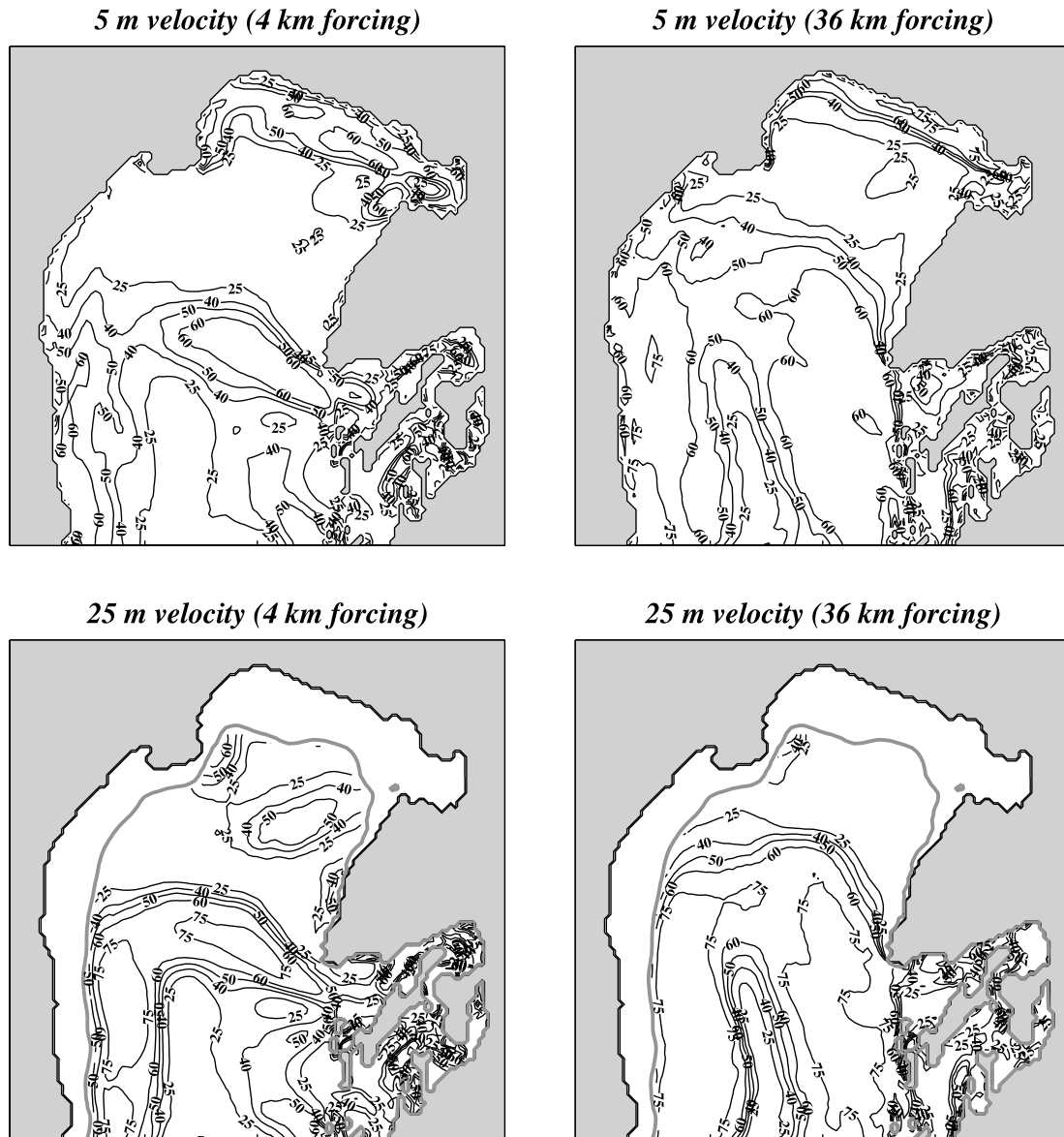
5 m velocity EOF 1 (4 km forcing)

5 m velocity EOF 1 (36 km forcing)

25 m velocity EOF 1 (4 km forcing)

25 m velocity EOF 1 (36 km forcing)

5 m velocity (4 km forcing)

5 m velocity (36 km forcing)

25 m velocity (4 km forcing)

25 m velocity (36 km forcing)

Figure 14. Percent local mean product explained by the velocity mode-1 EOFs displayed in Figure 13. Contours are 25, 40, 50, 60, and 75%.

smaller RMS errors of wind velocity than the 36-km model. The correlations of the 4- and 36-km modeled wind velocity with observed wind velocity were quite high (greater than 0.85) and were not dependent on the model resolution.

[52] Ocean model evaluation using two sites instrumented with ADCPs was conducted for the 4- and 36-km forced ocean model simulations. Variability with over twice the magnitude of the mean was observed and modeled at the shallow (UW) site. At most depths at the deeper (NRL) site the 36-km forced model yielded a stronger velocity mean and standard deviation of the principal component than the 4-km forced model. This increased magnitude of the mean and fluctuating currents accorded well with observations.

The 36-km forced model had smaller velocity RMS errors at both sites. Observed wind/current correlations at the NRL site increased down to approximately 20 m and then remained relatively depth-independent with values reaching in excess of 0.8. The 4-km forced model reproduced the shape and magnitude of the observed wind/current correlation as a function of depth better than the 36-km forced model. Below 20 m the 4-km forced model velocities correlated better with velocities observed at the NRL site.

[53] The wind stress curl mode-1 EOF of the 4-km COAMPS model displayed distinct regions of large negative wind stress curl that were absent in the 36-km COAMPS model. The UW and NRL observed 5-m major

Figure 13. (opposite) Velocity EOF 1 and amplitude time series at 5 and 25 m depths for the 4- and 36-km-resolution forced ocean models. The percent total mean product explained by the mode is given in each map.

Table 4. Maximum Correlation Coefficients and Associated Lag of EOF Mode-1 Wind Stress Curl and Ocean Current Amplitude Times Series

	Correlation Coefficient	Lag, Hours
4-km Forcing		
5-m current and wind stress curl	0.81	5
25-m current and wind stress curl	0.86	11
36-km Forcing		
5-m current and wind stress curl	0.80	8
25-m current and wind stress curl	0.83	12

axis velocity correlated most strongly with the regions of modeled maximum negative wind stress curl. Although the correlation between the observed 5-m ocean velocities at the two sites is below 0.2, the sites appear linked to some degree by expressing largest correlations with a common wind stress curl pattern.

[54] As demonstrated using an EOF analysis of the 4-km forced ocean model velocity along a section through the NRL ADCP site, below approximately 20 m depth the current over the 57-m isobath has an intensified wind forced response. The wind forcing also generates horizontal circulation (mapped using velocity EOFs at several depths) consisting of a double-gyre circulation when the 4-km-resolution COAMPS forcing is employed. The EOFs reveal this feature to be a generic ocean response to the applied high-resolution wind stress curl during the 125-day simulation. This pattern has appeared in observations (both remotely sensed and in situ) and some modeling simulations but is absent in our simulation using the 36-km-resolution COAMPS forcing. Hence the pattern of wind stress curl represented by the 4-km-resolution COAMPS model appears to produce more realistic circulation features in the ocean as well as better agreement with the observed correlation structure of winds with currents at the NRL site.

[55] *Munchow* [2000] presented observational evidence for the importance of small-scale atmospheric wind stress curl in inducing a cyclonic eddy in the underlying waters of the Santa Barbara Channel, California. Similarly, the wind stress curl over the northern Adriatic is linked to the double-gyre circulation in the shallow waters below. However, in addition, the energy of the bora is shown here to have an important effect on the ocean even at sites distant from the area of strongest applied atmospheric forcing. The mesoscale nonlocal air-ocean feedback documented here for the Adriatic region is likely an important component of other energetic coastal regions.

[56] In terms of seasonal effects, during winter and spring the northern Adriatic waters are quite homogeneous and currents are strongly wind-driven. The statistical analyses presented here show the models to be very capable of generating realistic levels of variability in the ocean during this time. During such barotropic conditions, variability travels along geostrophic contours, which isolates the middle part of the basin from the perimeter. When stratification effects become important during summer, baroclinic mean-

ders and instabilities of the boundary current may play a more pronounced role in the variability of the region.

[57] *Nachamkin and Hodur* [2000] conducted a validation study of the forecasts from two different resolution atmospheric COAMPS nests over the Mediterranean Sea. When computing error statistics for the two models, they encountered ambiguity in documenting the superior forecast capability afforded by the higher-resolution grid. They suggest that small phase and spatial errors may attend the higher-resolution forecasts, while limited validation data inhibit verification of spatial patterns. These factors do not necessarily render the higher-resolution models less skillful. Instead, they point to the need for more sophisticated verification tools as well as higher-resolution validation data.

[58] Although the RMS error of the 4-km model is smaller than the 36-km model at both observation sites, our work shows that the 4-km-resolution atmospheric model is not unambiguously superior to the 36-km-resolution model when correlations at individual observation points are compared. The Tolle and Pula stations are somewhat isolated from the main regions where the fine-scale structure of the bora is most evident (Figure 3). *Mass et al.* [2002] suggest that in locations where topography strongly controls the atmospheric flow, high-resolution models are capable of generating superior forecasts. However, in areas where the synoptic meteorology strongly controls the flow, information from the lateral boundaries (the coarser nest) can dominate the forecasts. The fact that the correlation coefficient between modeled and observed velocities at both Pula and Tolle is insensitive to the different model resolutions would indicate control to some extent of the two models by the shared synoptic meteorology; that is, the high modeled-observed correlations of comparable magnitudes produced by both the 4- and 36-km models may be a reflection of larger-scale influences that are common to both models.

[59] Nonetheless, at the two meteorological stations, the 36-km-resolution model substantially overpredicts the standard deviation of the principal component and yields a larger RMS error. Even over waters adjacent to the Pula and Tolle stations the ratio of the 36- to 4-km model wind stress variability exceeds 1.5 (Figure 3). Pula and Tolle are downstream from the mountainous region that accelerates the bora. Possibly due to some topographic control of the flow, the higher-resolution model is better able to predict the fluctuating winds at these locations. This hypothesis is reinforced by the correlation between Tolle and Pula winds, being largest for the 36-km model; that is, the 36-km model produces wind velocity time series at Tolle and Pula that are much more highly correlated with each other than are found in the 4-km model or observations, suggesting that aspects of the flow in topographically complex terrain that can be resolved on the 4-km grid allow the higher-resolution model to produce correlated but more distinguishable velocity time series at the two stations, as is observed.

[60] We have found that the higher-resolution atmospheric model produces velocity fields whose statistics are in better accordance with observations. Though the higher-resolution atmospheric model may be indistinguishable in its performance when correlated against point observations, the regional pattern of circulation produced on the higher-resolution grid is superior to its coarser-resolution counter-
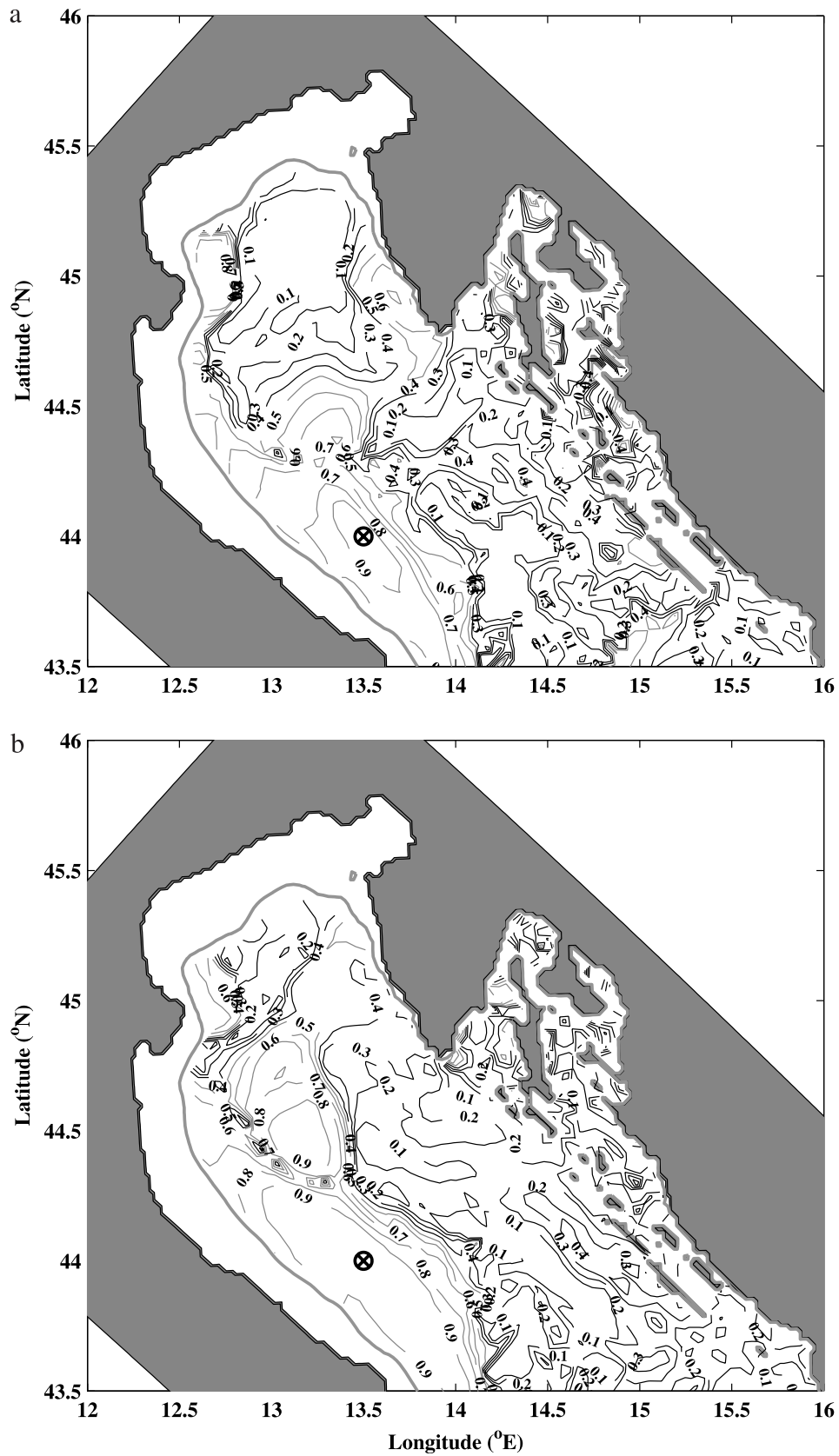
a

b

Figure 15. Maximum lagged correlations of modeled major axis velocity at 25 m depth at the NRL site for (a) the 4-km forced model and (b) the 36-km forced model with modeled major axis velocity at 25 m depth elsewhere in the model domain. Correlations are computed for every second model grid point. The NRL site is marked with a circled cross. Correlations of 0.5 and higher are shaded. Negative correlations have been set to zero.

part. The impact on the ocean is that certain statistical quantities at individual points removed from regions of strongest forcing appear relatively insensitive to, or even adversely affected by, the higher-resolution atmospheric forcing; while the regional patterns of coastal ocean circulation are quite favorably affected by the more refined imprint of wind stress curl left by the higher-resolution atmospheric model.

[61] Recent data assimilation efforts in the coastal ocean have utilized model-derived cross correlations to estimate the correlation structure of variables [*Oke et al.*, 2002; *Breivik and Saetra*, 2001]. Here major axis decorrelation scales are much longer for the Adriatic Sea simulation forced by the coarser-resolution COAMPS atmospheric model. This suggests that when determining decorrelation length scales for applications such as coastal ocean data assimilation, the scales generated by the ocean models might be highly dependent on the resolution of the atmospheric forcing. This is sure to become a more prominent issue as the ocean models gain higher resolution yet are limited in their ability to properly resolve scales of motion by the resolution of the atmospheric forcing.

References

Bergamasco, A., T. Oguz, and P. Malanotte-Rizzoli, Modeling dense water mass formation and winter circulation in the northern and central Adriatic Sea, *J. Mar. Syst.*, 20, 279–300, 1999.

Book, J. W., H. T. Perkins, L. Cavalieri, J. Doyle, and J. D. Pullen, ADCP observations of the western Adriatic slope current during winter of 2001, *Prog. Oceanogr*, in press, 2003.

Bougeault, P., P. Binder, A. Buzzi, R. Dirks, R. Houze, J. Kuettner, R. B. Smith, R. Steinacker, and H. Volkert, The MAP special observing period, *Bull. Am. Meteorol. Soc.*, 82, 433–462, 2001.

Breivik, O., and O. Saetra, Real time assimilation of HF radar currents into a coastal ocean model, *J. Mar. Syst.*, 28, 161–182, 2001.

Cushman-Roisin, B., and C.E. Naimie, A 3D finite-element model of the Adriatic tides, *J. Mar. Syst.*, 37, 279–297, 2002.

Hodur, R. M., The Naval Research Laboratory's Coupled Ocean/Atmosphere Mesoscale Prediction System (COAMPS), *Mon. Weather Rev.*, 125, 1414–1430, 1997.

Hodur, R. M., J. Pullen, J. Cummings, X. Hong, J. D. Doyle, P. Martin, and M. A. Rennick, The Coupled Ocean/Atmosphere Mesoscale Prediction System (COAMPS), *Oceanography*, 15, 88–98, 2001.

Kondo, J., Air-sea bulk transfer coefficients in diabatic conditions, *Boundary Layer Meteorol.*, 9, 91–112, 1975.

Kourafalou, V., River plume development in semi-enclosed Mediterranean regions: North Adriatic Sea and Northwest Aegean Sea, *J. Mar. Syst.*, 30, 181–205, 2001.

Kourafalou, V. H., L.-Y. Oey, J. D. Wang, and T. N. Lee, The fate of river discharge on the continental shelf: 1. Modeling the river plume and the inner-shelf coastal current, *J. Geophys. Res.*, 101(C2), 3415–3434, 1996.

Kuzmic, M., and M. Orlic, Wind-induced vertical shearing: ALPEX/MEDALPEX data and modeling exercise, *Ann. Geophys., Ser. B.*, 5, 103–112, 1987.

Martin, P. J., A description of the Navy Coastal Ocean Model version 1.0, *Nav. Res. Lab. Rep. NRL/FR/7322-00-9962*, 42 pp., Nav. Res. Lab., Stennis Space Cent., Miss., 2000.

Martin, P. J., and R. M. Hodur, Mean COAMPS air-sea fluxes over the Mediterranean during 1999, report, Nav. Res. Lab., Stennis Space Center, Miss., in press, 2003.

Mass, C. F., D. Ovens, K. Westrick, and B. A. Colle, Does increasing horizontal resolution produce more skillful forecasts? The results of two years of real-time numerical weather prediction over the Pacific Northwest, *Bull. Am. Meteorol. Soc.*, 83, 407–430, 2002.

Mauri, E., and P.-M. Poulain, Northern Adriatic Sea surface circulation and temperature/pigment fields in September and October 1997, *J. Mar. Syst.*, 29, 51–67, 2001.

Mellor, G. L., T. Ezer, and L.-Y. Oey, The pressure gradient conundrum of sigma coordinate ocean models, *J. Atmos. Oceanic Technol.*, 11, 1126–1134, 1994.

Munchow, A., Wind stress curl forcing of the coastal ocean near Point Conception, California, *J. Phys. Oceanogr.*, 30, 1265–1280, 2000.

Nachamkin, J. E., and R. M. Hodur, Verification of short-term forecasts from the Navy COAMPS over the Mediterranean, paper presented at 15th Conference on Statistics and Probability in the Atmospheric Sciences, Am. Meteorol. Soc., Asheville, N. C., 2000.

Nelson, B., Hydrography, sediment dispersal, and recent historical development of the Po River delta, Italy, in *Deltaic Sedimentation Modern and Ancient, Spec. Publ. SEPM Soc. Sediment. Geol.*, 15, 152–184, 1970.

Oke, P. R., J. S. Allen, R. N. Miller, G. D. Egbert, and P. M. Kosro, Assimilation of surface velocity data into a primitive equation coastal ocean model, *J. Geophys. Res.*, 107(C9), 3122, doi:10.1029/2000JC000511, 2002.

Orlic, M., M. Kuzmic, and Z. Pasaric, Response of the Adriatic Sea to the bora and sirocco forcing, *Cont. Shelf Res.*, 14, 91–116, 1994.

Paklar, G. B., V. Isakov, D. Koracin, V. Kourafalou, and M. Orlic, A case study of bora-driven flow and density changes on the Adriatic Shelf (January 1987), *Cont. Shelf Res.*, 21, 1751–1783, 2001.

Perry, G. D., P. B. Duffy, and N. L. Miller, An extended data set of river discharge for validation of general circulation models, *J. Geophys. Res.*, 101(D16), 21,339–21,349, 1996.

Poulain, P., Adriatic Sea surface circulation as derived from drifter data between 1990 and 1999, *J. Mar. Syst.*, 29, 3–32, 2001.

Raicich, F., Note on the flow rates of the Adriatic rivers, *Tech. Rep. RF 02/94*, 8 pp., CNR Ist. Sper. Talassografico, Trieste, Italy, 1994.

Rochford, P. A., and P. J. Martin, Boundary conditions in the Navy Coastal Ocean Model, *Rep. NRL/FR/7330-01-9992*, 33 pp., Nav. Res. Lab., Stennis Space Cent., Miss., 2001.

Signell, R. P., S. Carniel, L. Cavalieri, J. Chiaggiato, J. Doyle, J. Pullen, and M. Selavo, Assessment of wind quality for oceanographic modeling in semi-enclosed basins, *J. Mar. Syst.*, in press, 2003.

Smith, R. B., Aerial observations of the Yugoslavian bora, *J. Atmos. Sci.*, 44, 269–297, 1987.

Sturm, B., M. Kuzmic, and M. Orlic, An evaluation and interpretation of CZCS-derived patterns on the Adriatic shelf, *Oceanol. Acta*, 15, 13–23, 1992.

Supic, N., M. Orlic, and D. Degobbis, Istrian coastal countercurrent and its year-to-year variability, *Estuarine Coastal Shelf Sci.*, 51, 385–397, 2000.

Zavatarelli, M., and N. Pinardi, The Adriatic Sea modeling system: A nested approach, *Ann. Geophys.*, 21, 345–364, 2003.

Zavatarelli, M., N. Pinardi, V. H. Kourafalou, and A. Maggiore, Diagnostic and prognostic model studies of the Adriatic Sea general circulation: Seasonal variability, *J. Geophys. Res.*, 107(C1), 3004, doi:10.1029/2000JC000210, 2002.

Zore-Armanda, M., and M. Gacic, Effects of bura on the circulation in the northern Adriatic, *Ann. Geophys., Ser. B.*, 5, 93–102, 1987.

————————————
J. W. Book and H. Perkins, Naval Research Laboratory, Stennis Space Center, MS 39529, USA. (book@nrlssc.navy.mil; hperkins@nrlssc.navy.mil)

J. D. Doyle, R. Hodur, and J. Pullen, Marine Meteorology Division, Naval Research Laboratory, 7 Grace Hopper Avenue, Stop 2, Monterey, CA 93943, USA. (doyle@nrlmry.navy.mil; hodur@nrlmry.navy.mil; pullen@nrlmry.navy.mil)

A. Ogston, School of Oceanography, University of Washington, Seattle, WA 98195, USA. (ogston@ocean.washington.edu)

R. Signell, SACLANT Undersea Research Centre, Viale San Bartolomeo 400, I-19138 La Spezia, Italy. (signell@saclantc.nato.int)